Chiral fermion meson model at finite temperature

H. C. G. Caldas*,
Departamento de Ciências Naturais, DCNAT Fundação de Ensino Superior de São João del Rei, FUNREI, Praça Dom Helvécio, 74, CEP:36300-000, São João del Rei, MG, Brazil and Departamento de Física, Universidade Federal de Minas Gerais, CP 702, CEP:30.161-970, Belo Horizonte, MG, Brazil

A. L. Mota
Departamento de Ciências Naturais, DCNAT Fundação de Ensino Superior de São João del Rei, FUNREI, Praça Dom Helvécio, 74, CEP:36300-000, São João del Rei, MG, Brazil

M. C. Nemes
Departamento de Física, Universidade Federal de Minas Gerais, CP 702, CEP:30.161-970, Belo Horizonte, MG, Brazil

(Received 18 May 2000; published 8 February 2001)

We study the chiral fermion meson model which is the well-known linear sigma model of Gell-Mann and Levy at finite temperature. A modified self-consistent resummation (MSCR) which resums higher order terms in the perturbative expansion is proposed. It is shown that with the MSCR the problem of tachyonic masses is solved, the renormalization of the gap equations is carried out, and Goldstone's theorem is verified. We also apply the method to investigate another known case at high temperature and compare with results found in the literature.

DOI: 10.1103/PhysRevD.63.056011 PACS number(s): 11.10.Wx, 11.30.Rd, 12.39.−x

I. INTRODUCTION

Several models have been proposed to describe hadron properties in the regime of low energies. Among these models, we adopt the linear σ model of Gell-Mann and Levy [1] which is a phenomenological model of quantum chromodynamics (QCD) that incorporates two important features of QCD: chiral symmetry and partial conservation of axial vector current PCAC. The model was originally proposed as a model for strong interactions [1], but nowadays it serves as an effective model for the low-energy (low-temperature) phase of QCD. It has the advantage of being renormalizable at zero [2] and finite temperature [3]. Although the linear sigma model Lagrangian exhibits chiral symmetry, quantum effects break this symmetry spontaneously. Both from theoretical [4] and experimental [5] points of view, there exists a great amount of interest in the study of chiral symmetry restoration at finite temperature.

However, quantum field theory at high temperature has a well known problem, that is, the breakdown of the perturbative expansion [6–8]. This happens in theories with spontaneous symmetry breaking (SSB) or in massless field theories because powers of the temperature can compensate for powers of the coupling constant. Resummation techniques which try consistently to take into account higher loops are required.

A systematic self-consistent approximation approaches based on the meson sector of the linear σ model was previously studied by Baym and Grinstein [9]. After, Banerjee and Mallik [10] proposed a modified perturbation expansion with the objective of calculating the two-point functions up to second order in the $\lambda\phi^4$ theory. A resummed perturbative expansion was proposed by Parwani [11] in order to go beyond leading order in the same model. More recently, Chiku and Hatsuda [12] in the study of the $O(N)$ ϕ^4 model presented a novel resummation adding a mass parameter determined later by the fastest apparent convergence (FAC) condition. We employ imaginary-time formulation (ITF) whereas in [12] real-time formulation (RTF) is used in the development of the optimized perturbation theory (OPT). In this paper we develop a modified self-consistent resummation at finite temperature and apply it to the investigation of the chiral fermion meson model. We study the temperature dependence of the chiral condensate and the effective meson and fermion masses by this self-consistent nonperturbative approximation up to one-loop order in the perturbative expansion. In the application of the modified self-consistent resummation (MSCR) to the study of the chiral fermion meson model at finite temperature, we divided the problem into three physical regions: low, intermediate, and high temperatures. This is essential to identify the regions where resummation is crucial. In each region renormalization and satisfaction of Goldstone's theorem are discussed in detail. Our study addresses problems found in the context of the well studied $O(4)$ linear sigma model and deals with a usually avoided point: the inclusion of the fermions. Also, we reexamine the chiral phase transition in static equilibrium in terms of the linear sigma model with our MSCR. Instead of demanding an infinite gap equation, as has been done often in the recent literature, we perform the renormalization in stages in order to get finite gap equations.

We also treat an explicit chiral symmetry breaking term in the Lagrangian which generates the realistic finite pion mass. Symmetry is never restored in this case. It is shown that in the limit of vanishing pion mass, namely, when the chiral symmetry is exact, the inclusion of fermions does not change the order (nature) of the phase transition but only lowers the

*Email address: hcaldas@funrei.br

value of the critical temperature.

This paper is organized as follows. In Sec. II we discuss the chiral fermion meson model and some of its features at zero temperature. In Sec. III the temperature is introduced via the partition function of the model which lead to the thermodynamical potential. The inclusion of loop corrections and the thermal gap equations are addressed to Sec. IV. In Sec. V we apply the MSCR to the study of the massless $\lambda\phi^4$ model in the weak coupling limit at high temperature. The renormalization of the self-energy is studied in Sec. VI. The numerical results are presented in Sec. VII. Section VIII is devoted to conclusions.

II. THE CHIRAL FERMION MESON MODEL AT ZERO TEMPERATURE

The Lagrangian density of the chiral fermion meson model which provides an explicit realization of chiral symmetry is given by [1]

$$\mathcal{L}_{sym}=\bar{\psi}[i\gamma^\mu\partial_\mu-g(\sigma'+i\gamma^5\vec{\pi}\cdot\vec{\tau})]\psi+\frac{1}{2}[(\partial\sigma')^2+(\partial\vec{\pi})^2]$$

$$-\frac{\lambda}{4}(\sigma'^2+\vec{\pi}^2-f_\pi^2)^2, \tag{1}$$

where ψ, σ', and π represent the quark, sigma, and pion fields, respectively, λ and g are positive coupling constants, and f_π is the pion decay constant in vacuum.

If the up and down quark masses were zero, QCD would have a chiral $SU(2)_L\times SU(2)_R$ symmetry. In the vacuum this symmetry is spontaneously broken by quantum effects, with the result that there exists a triplet of Goldstone bosons. In reality the quark masses are very small but nonzero, so that chiral symmetry is only approximate and the pion has a small mass [13]. An explicit chiral symmetry breaking term is added to the Lagrangian which generates the realistic finite pion mass so that

$$\mathcal{L}'=\mathcal{L}_{\rm sym}+\mathcal{L}_{\rm symb}, \tag{2}$$

with

$$\mathcal{L}_{\rm symb}=c\sigma', \tag{3}$$

where c is small and positive.

The term $\mathcal{L}_{\rm sym}$ is symmetric and invariant under a $SU(2)_L\times SU(2)_R$ chiral group and $\mathcal{L}_{\rm symb}$ is the symmetry breaking term. Two Noether currents associated with Eq. (1), namely, the vector current and the axial vector current, are given by

$$\vec{V}_\mu=\bar{\psi}\gamma_\mu\frac{\vec{\tau}}{2}\psi+\vec{\pi}\times\partial_\mu\vec{\pi},$$

$$\vec{A}_\mu=\bar{\psi}\gamma_\mu\gamma_5\frac{\vec{\tau}}{2}\psi+\sigma'\partial_\mu\vec{\pi}-\vec{\pi}\partial_\mu\sigma',$$

respectively. The equations of motion for the fields derived from the Lagrangian density (1) give the PCAC relations

$$\partial_\mu\vec{A}^\mu=c\vec{\pi}. \tag{4}$$

The effect of the term $c\sigma'$ on the classical fundamental state can be found by looking at the minimum of the potential

$$V_0(\sigma',\vec{\pi})=\frac{\lambda}{4}(\sigma'^2+\vec{\pi}^2-f_\pi^2)^2-c\sigma', \tag{5}$$

$$\frac{\partial V_0(\sigma',\vec{\pi})}{\partial\sigma'}=\lambda(\sigma'^2+\vec{\pi}^2-f_\pi^2)\sigma'-c=0, \tag{6}$$

$$\frac{\partial V_0(\sigma',\vec{\pi})}{\partial\pi^a}=\lambda(\sigma'^2+\vec{\pi}^2-f_\pi^2)\pi^a=0 \tag{7}$$

whose (unique) solutions are

$$\vec{\pi}_0=0,$$

$$\lambda(\sigma_0'^2-f_\pi^2)\sigma_0'=c. \tag{8}$$

To first order in c, we have

$$\sigma_0'=f_\pi+\frac{c}{2\lambda f_\pi^2}\equiv\nu. \tag{9}$$

From Eq. (9), we see that σ_0' has a nonzero vacuum expectation value. It is convenient to redefine the sigma field as $\sigma'\to\sigma+\nu$ such that σ has zero expectation value. As an effect of this shift the fermion field acquires a mass given by

$$m_\psi=g\nu. \tag{10}$$

The shifted Lagrangian, $\mathcal{L}_s$, of the new quantum theory reads

$$\mathcal{L}_s=-\frac{\lambda}{4}(f_\pi^2-\nu^2)^2+c\nu-\lambda\left(\nu^3-\nu f_\pi^2-\frac{c}{\lambda}\right)\sigma$$

$$+\bar{\psi}[i\gamma^\mu\partial_\mu-m_\psi]\psi+\frac{1}{2}[(\partial\vec{\pi})^2-m_\pi^2\vec{\pi}^2$$

$$+(\partial\sigma)^2-m_\sigma^2\sigma^2]-g\bar{\psi}[\sigma+i\gamma^5\vec{\pi}\cdot\vec{\tau})]\psi$$

$$-\frac{\lambda}{4}[(\vec{\pi}^2+\sigma^2)^2+4\nu\sigma(\vec{\pi}^2+\sigma^2)]$$

$$=-U(\nu)+\mathcal{L}_0+\mathcal{L}_I, \tag{11}$$

where $U(\nu)$ is the mean field energy density, $\mathcal{L}_0$ is the free Lagrangian, and $\mathcal{L}_I$ is the interaction Lagrangian, defined by

$$U(\nu)\equiv\frac{\lambda}{4}(f_\pi^2-\nu^2)^2-c\nu, \tag{12}$$

$$\mathcal{L}_0\equiv\bar{\psi}[i\gamma^\mu\partial_\mu-m_\psi]\psi+\frac{1}{2}[(\partial\vec{\pi})^2$$

$$-m_\pi^2\vec{\pi}^2+(\partial\sigma)^2-m_\sigma^2\sigma^2], \tag{13}$$

$$\mathcal{L}_I \equiv -g\bar{\psi}[\sigma + i\gamma^5 \vec{\pi}\cdot\vec{\tau})]\psi - \frac{\lambda}{4}[(\vec{\pi}^2+\sigma^2)^2 + 4\nu\sigma(\vec{\pi}^2+\sigma^2)], \quad (14)$$

respectively.

The meson masses read out of the shifted Lagrangian (11) are

$$m_\pi^2 = m^2 + \lambda\nu^2, \quad (15)$$

$$m_\sigma^2 = m^2 + 3\lambda\nu^2, \quad (16)$$

where $m^2 = -\lambda f_\pi^2 < 0$. It is easy to see that the coefficient of the linear term in the sigma field $\lambda(\nu^3 - \nu f_\pi^2 - c/\lambda)$ in Lagrangian (11) is identically zero by the minimal condition (8). This is due to the fact that the vacuum expectation value of the sigma field $\langle\sigma\rangle$ should vanish at any order of perturbation theory [14], even if we include thermal corrections [15]. The one-loop thermal tadpole corrections will modify this relation which will become temperature dependent. If ν is allowed to be temperature dependent, the masses are temperature dependent as well. At any temperature, ν is such that $\langle\sigma\rangle = 0$. At zero temperature, when c continuously approaches zero, we have the solutions $\langle\vec{\pi}\rangle = 0$ and $\langle\sigma'\rangle = f_\pi$ which minimize the potential satisfying Goldstone's theorem.

The contact with phenomenology is made by fixing the parameters of the model to agree with the observable value of the particle masses in vacuum. Then, the tree level parameters of the Lagrangian are

$$\lambda = \frac{m_{\sigma;0}^2 - 3m_{\pi;0}^2}{2f_\pi^2}, \quad (17)$$

$$c = \nu m_{\pi;0}^2 \simeq f_\pi m_{\pi;0}^2, \quad (18)$$

$$g = \frac{m_{\psi;0}(m_{\sigma;0}^2 - 3m_{\pi;0}^2)}{f_\pi(m_{\sigma;0}^2 - 2m_{\pi;0}^2)}, \quad (19)$$

where $m_{\pi;0} = 139$ MeV, $m_{\sigma;0} = 600$ MeV, $m_{\psi;0} = 340$ MeV, and $f_\pi = 93$ MeV.

As we mentioned earlier, our goal in this work is to study the chiral phase transition in the chiral fermion meson model and to analyze the thermal behavior of the temperature dependent meson condensate ν and the meson and fermion masses. So it will be necessary to compute all the one-loop self-energies for the particles present in the model. Such self-energy diagrams have divergent pieces which must be renormalized if we want reliable results. In most of the approximations found in the literature [9,16–18] several difficulties have been found in the tentative of renormalizing the divergent gap equations. Sometimes the undesirable parts have been ignored [19]. The renormalization of the self-energy is studied in Sec. VI whereas the effective potential renormalization is performed in Appendix A. For the purpose of renormalization it is necessary to add to $\mathcal{L}_s$ a counterterm (CT) Lagrangian $L_{\rm CT}$, needed to render the theory finite [20],

$$\mathcal{L} = \mathcal{L}_s + L_{\rm CT}, \quad (20)$$

where

$$L_{\rm CT} = {\rm CT} + D_1 m_\psi^4 + D_2 m_\pi^4 + D_3 m_\sigma^4. \quad (21)$$

In Eq. (21) CT contains the appropriate counterterms to be used in the renormalization of the masses while $D_{1,2,3} m_{\psi,\pi,\sigma}^4$ are necessary to keep the thermodynamical potential finite, as we will see further. As we are interested only in the study of the thermal effective masses at one loop order in the perturbative expansion, other counterterms necessary to renormalize the coupling constants are not explicitly shown.

III. THE PARTITION FUNCTION OF THE MODEL AND THE LINK TO STATISTICAL MECHANICS

One of the most fundamental objects in thermodynamics is the partition function, defined by

$$Z = {\rm Tr}\, e^{-\beta\hat{H}}, \quad (22)$$

where $\hat{H}$ is the Hamiltonian of the system, $\beta = 1/k_B T = T^{-1}$ with the Boltzmann constant k_B set equal to 1 and the trace (Tr), in Eq. (22) meaning the sum of the elements of the matrix $e^{-\beta\hat{H}}$ in all independent states of the system. All information concerning the equilibrium thermodynamic macroscopic properties of the system are obtained from Z.

In relativistic quantum field theory, the partition function can be derived from the Feynman's functional formalism [21]. The bridge between quantum mechanics and statistical mechanics is achieved by the Heuristic introduction of a variable defined as $\tau = it$. Also, the fields are constrained to obey periodic (anti) boundary conditions $\phi(\mathbf{r},0) = \phi(\mathbf{r},\beta)$ for bosons and $\psi(\mathbf{r},0) = -\psi(\mathbf{r},\beta)$ for fermions. Following these prescriptions, we get

$$Z[\bar{\psi},\psi,\sigma,\pi] = N' \int \mathcal{D}[\phi] \exp\left[\int_0^\beta d\tau \int d^3x\, \mathcal{L}(\phi,\partial\phi)\right] = \exp\int_\beta d^4x \left[-\frac{\lambda}{4}(f_\pi^2 - \nu^2)^2 + c\nu + D_1 m_\psi^4 + D_2 m_\pi^4 + D_3 m_\sigma^4\right] N' \int \mathcal{D}[\phi] e^{S_0} e^{S_I}. \quad (23)$$

Here we have introduced a short hand notation for the Euclidean space-time integral $S = \int_\beta d^4x\, \mathcal{L} \equiv \int_0^\beta d\tau \int d^3x\, \mathcal{L}$, $\mathcal{D}[\phi]$ is an abbreviation for the integral over $\bar{\psi}$, ψ, σ, and π, N' is an unimportant infinite constant, and $\mathcal{L}$ is given by Eq. (20).

Next we introduce the thermodynamical potential Ω defined by

$$\Omega(T,\nu) = -\frac{T}{V}\ln Z, \tag{24}$$

where $\ln Z = (V/T)[U(\nu) + D_{1,2,3} m^4_{\psi,\pi,\sigma}] + \ln Z_0 + \ln Z_I$. Since the interaction action S_I contains terms which are more than quadratic in the fields, it is not possible to carry out the functional integration above in closed form. For a while we will neglect S_I in our calculations. This amounts to considering only the tadpole contributions. Thus,

$$\begin{aligned}
\Omega_1(T,\nu) &\equiv \frac{\lambda}{4}(f_\pi^2 - \nu^2)^2 - c\nu \\
&\quad - [D_1 m_\psi^4 + D_2 m_\pi^4 + D_3 m_\sigma^4] - \frac{T}{V}\ln Z_0 \\
&= \frac{\lambda}{4}(f_\pi^2 - \nu^2)^2 - c\nu - [D_1 m_\psi^4 + D_2 m_\pi^4 + D_3 m_\sigma^4] \\
&\quad + \int \frac{d^3p}{(2\pi)^3}\left\{\frac{1}{2}\omega_\sigma + T\ln(1 - e^{-\beta\omega_\sigma})\right. \\
&\quad + \frac{3}{2}\omega_\pi + 3T\ln(1 - e^{-\beta\omega_\pi}) \\
&\quad \left. - 2\times 2[\omega_\psi + 2T\ln(1 + e^{-\beta\omega_\psi})]\right\}
\end{aligned} \tag{25}$$

with $\omega_\sigma^2 \equiv \mathbf{p}^2 + m_\sigma^2$, $\omega_\pi^2 \equiv \mathbf{p}^2 + m_\pi^2$, and $\omega_\psi^2 \equiv \mathbf{p}^2 + m_\psi^2$. In the third line of Eq. (25) the first factor 2 multiplying the bracket which contains the fermion contribution, comes from the spin degrees of freedom, whereas the other factor two is due the isospin degrees of freedom. Inside this same bracket there is another factor 2 corresponding to the particle and antiparticle contributions. The thermodynamical potential Ω_1 is precisely the one-loop effective potential [6,3] of the linear sigma model, and it can be expressed as

$$\Omega_1(T,\nu) = U(\nu) + D_{1,2,3} m^4_{\psi,\pi,\sigma} + \Omega_1^0(\nu) + \Omega_1^\beta(T,\nu). \tag{26}$$

The equation of state of the noninteracting system composed by a (free) relativistic boson and fermion gas is

$$\begin{aligned}
P_0 &= \frac{T}{V}\ln Z_0 = -\Omega_1^\beta(T,\nu) \\
&= -T\int \frac{d^3p}{(2\pi)^3}[\ln(1 - e^{-\beta\omega_\sigma}) \\
&\quad + 3\ln(1 - e^{-\beta\omega_\pi}) - 8\ln(1 + e^{-\beta\omega_\psi})],
\end{aligned} \tag{27}$$

where P_0 is the thermal pressure.

The integration over the temperature independent terms $\Omega_1^0(\nu) \equiv \int [d^3p/(2\pi)^3][\frac{1}{2}\omega_\sigma + \frac{3}{2}\omega_\pi - 4\omega_\psi]$ actually diverges. It is exactly the counterterms $D_{1,2,3} m^4_{\psi,\pi,\sigma}$ which will take care of these divergences. We discuss this further in Sec. VI. It can be known, from thermodynamical considerations, that in thermal equilibrium Ω is a minimum with respect to variations in ν [13]. Applying this extremum condition, we have

$$\frac{\partial\Omega_1(T,\nu)}{\partial\nu} = 0. \tag{28}$$

Since $\Omega_1^\beta(T=0,\nu) = 0$, the divergent quantity $\partial\Omega_1^0(\nu)/\partial\nu = \int [d^3p(2\pi)^3][3\lambda(1/2\omega_\sigma + 1/2\omega_\pi) - 8g^2(1/2\omega_\psi)]\nu$ represents the sum of the tadpoles at $T=0$. On the other hand, $\partial\Omega_1^\beta(T,\nu)/\partial\nu$ is finite at $T \neq 0$ because of the natural cutoff $1/[(e^{\beta\omega_{\sigma\pi,(\psi)}} - (+)1)]$ present in the integrals. We could let the counterterms absorb the finite parts of $\partial\Omega_1^0(\nu)/\partial\nu$ together with the infinities since the vacuum contribution is irrelevant for the discussions of thermodynamics. But, as we will see in Sec. IV C, these terms are important in the verification of the Goldstone theorem in our self-consistent treatment. After these considerations, Eq. (28) is written as

$$\begin{aligned}
&\{F[\omega_{\pi,\sigma,\psi}(m_{\pi,\sigma,\psi}), T] + G[\omega_{\pi,\sigma,\psi}(m_{\pi,\sigma,\psi})] \\
&\quad - \lambda(f_\pi^2 - \nu^2)\}\nu - c = 0,
\end{aligned} \tag{29}$$

where the functions F and G are defined as

$$\begin{aligned}
&F[\omega_{\pi,\sigma,\psi}(m_{\pi,\sigma,\psi}), T] \\
&\quad \equiv \int \frac{d^3p}{(2\pi)^3}\left[3\lambda\left(\frac{1}{\omega_\sigma(e^{\beta\omega_\sigma} - 1)} + \frac{1}{\omega_\pi(e^{\beta\omega_\pi} - 1)}\right)\right. \\
&\quad \left. + 8g^2\frac{1}{\omega_\psi(e^{\beta\omega_\psi} + 1)}\right],
\end{aligned} \tag{30}$$

$$\begin{aligned}
&G[\omega_{\pi,\sigma,\psi}(m_{\pi,\sigma,\psi})] \\
&\quad \equiv \frac{3\lambda}{(4\pi)^2}\left[m_\pi^2\ln\left(\frac{m_\pi^2}{\mu^2}\right) + m_\sigma^2\ln\left(\frac{m_\sigma^2}{\mu^2}\right)\right] \\
&\quad - \frac{8g^2}{(4\pi)^2}m_\psi^2\ln\left(\frac{m_\psi^2}{\mu^2}\right),
\end{aligned} \tag{31}$$

respectively. In Eq. (31), μ is the renormalization scale.

As a first approximation, we consider only the thermal loop corrections to the effective potential. This approximation allows us to get an analytic expression for the approximate critical temperature:

$$\begin{aligned}
&\int \frac{d^3p}{(2\pi)^3}\left[3\lambda\left(\frac{n_\pi(\omega_\pi)}{\omega_\pi} + \frac{n_\sigma(\omega_\sigma)}{\omega_\sigma}\right)\right. \\
&\quad \left. + 8g^2\frac{n_\psi(\omega_\psi)}{\omega_\psi}\right]\nu - \lambda(f_\pi^2 - \nu^2)\nu - c = 0,
\end{aligned} \tag{32}$$

where $n_{\pi,\sigma}$ and n_ψ are the usual distribution functions for bosons and fermions given by

$$n_{\pi,\sigma}(\omega_{\pi,\sigma}; T) = \frac{1}{e^{\beta\omega_{\pi,\sigma}} - 1}, \tag{33}$$

$$n_\psi(\omega_\psi;T)=\frac{1}{e^{\beta\omega_\psi}+1}, \tag{34}$$

respectively. In the above expression, when one minimizes the effective potential, one is summing the thermal tadpole contributions to the usually called mean field equation. The chiral condensate ν, which is a nontrivial solution of this integral equation now depends on T. This equation can be solved with an explicit analytic form in the high-temperature limit. The leading terms in the high-temperature approximation for this integral equation are

$$\nu^3+\left[\frac{1}{2}\left(1+\frac{2g^2}{3\lambda}\right)T^2-f_\pi^2\right]\nu-\frac{c}{\lambda}=0. \tag{35}$$

The above equation has a real solution that is a slowly decreasing function of temperature, but does not vanish. Thus, when $c\neq 0$ the symmetry is never restored. On the other hand, when $c=0$ the nontrivial solution of Eq. (35) is

$$\nu^2=f_\pi^2-\frac{1}{2}\left(1+\frac{2g^2}{3\lambda}\right)T^2. \tag{36}$$

The critical temperature is defined as the temperature where the condensate goes to zero. It is given by

$$T_c^2=\frac{2f_\pi^2}{(1+2g^2/3\lambda)}. \tag{37}$$

It shows that the inclusion of fermions does not change the order of the phase transition, but only lowers the value of T_c. Note that the interactions of the mesons with the fermions forces the ''critical'' temperature to depend on the coupling constants λ and g. If $g=0$ we recover the result of Ref. [22].

IV. INCLUSION OF LOOP CORRECTIONS

A. The first necessity: Beyond the mean field approximation

Let us analyze the finite temperature behavior of the tree-level meson masses (15) and (16) as functions of the thermal expectation value of the sigma field $\nu(T)$. Since $\nu^2(T)$ decreases as T increases and $m^2<0$, the particle masses become tachyonic. Another problem which arises is the fact that Goldstone's theorem is not satisfied in the ordered phase (when $c=0$), i.e., replacing Eq. (36) in Eq. (15), we obtain a nonzero pion mass given by $m_\pi^2=-(\lambda/2)(1+2g^2/3\lambda)T^2$. This pathological behavior is due to the fact that in our approximation we have neglected the interaction action S_I in the thermodynamical potential (24). The result is that the mean field approximation can be trusted only in the approximate prediction of a phase transition at T_c given by Eq. (37). It is incorrect in what concern the description of the finite temperature behavior of the meson and fermion masses. So it is necessary to include all one-loop corrections from all one particle irreducible (1PI) diagrams present in S_I to the masses.

Following the program of [13] we expand the partition function in powers of the interaction, in order to get the one-loop self-energy corrections:

$$\ln Z_I=\ln\left(1+\sum_{n=1}^{\infty}\frac{1}{n!}\frac{\int[d\phi]e^{S_0}S_I^n}{[d\phi]e^{S_0}}\right). \tag{38}$$

The one-loop 1PI graphs come from $\ln Z_1+\ln Z_2$, which are given by

$$\ln Z_1=\frac{\int[d\phi]e^{S_0}S_I}{[d\phi]e^{S_0}}, \tag{39}$$

$$\ln Z_2=-\frac{1}{2}\left(\frac{\int[d\phi]e^{S_0}S_I}{[d\phi]e^{S_0}}\right)^2+\frac{1}{2}\frac{\int[d\phi]e^{S_0}S_I^2}{[d\phi]e^{S_0}}, \tag{40}$$

where the disconnected diagrams cancel in $\ln Z_2$ and the diagrams which gives rise to tadpoles in the self-energy are not to be included, since their effect is already considered in the mean field equation. The terms which ''survive'' come from

$$\ln Z_I^{2\text{-loop}}=-\frac{\lambda}{4}\frac{\int[d\phi]e^{S_0}\int d\tau\int d^3x(\pi^2+\sigma^2)^2}{\int[d\phi]e^{S_o}}$$

$$+\frac{1}{2}\int_0^\beta d\tau_1\,d\tau_2\int d^3x_1\,d^3x_2\frac{\int[d\phi]e^{S_0}\{\lambda^2\nu^2[(\sigma\pi^2)^2+(\sigma^3)^2]+g^2[(\bar\psi\sigma\psi)^2+(\bar\psi i\gamma^5\vec\pi\cdot\vec\tau\psi)^2]\}}{\int[d\phi]e^{S_0}}. \tag{41}$$

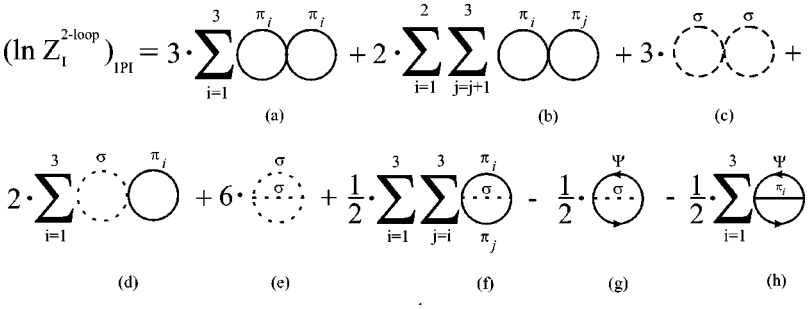

FIG. 1. The logarithm of the interaction partition function 1PI. The solid line is the tree-level pion meson propagator, the dashed line is the tree-level sigma meson propagator, and the solid line with an arrow is the tree-level fermion propagator.

The 1PI graphs from this expression can be represented diagrammatically as shown in Fig. 1.

The self-energy for bosons and fermions are defined, respectively, by

$$\mathbf{D}(\omega_n,\mathbf{k})^{-1}_{\sigma,\pi}=\mathbf{D}_{0\sigma,\pi}(\omega_n,\mathbf{k})^{-1}+\Pi_{\sigma,\pi}(\omega_n,\mathbf{k}), \tag{42}$$

$$\mathcal{D}(\omega_n,\mathbf{k})^{-1}=\mathcal{D}_0(\omega_n,\mathbf{k})^{-1}+\Sigma(\omega_n,\mathbf{k}), \tag{43}$$

where $\mathbf{D}_{0\sigma,\pi}(\omega_n,\mathbf{p})$ and $\mathcal{D}_0(\omega_n,\mathbf{p})$ are the tree-level boson and fermion propagators, expressed, respectively, as

$$\mathbf{D}_{0\sigma,\pi}(\omega_n,\mathbf{k})^{-1}=\omega_n^2+\mathbf{k}^2+m^2_{\sigma,\pi}, \tag{44}$$

$$\mathcal{D}_0(\omega_n,\mathbf{k})^{-1}=\gamma_\mu k^\mu-m_\psi. \tag{45}$$

Here, ω_n are the Matsubara frequencies, defined as $\omega_n=2n\pi T$ for bosons and $\omega_n=(2n+1)\pi T\equiv\omega_{nf}$ for fermions.

To one-loop order the self-energy expressions are given [13] by

$$\Pi_{\sigma,\pi}=-2\left(\frac{\delta\ln Z_I^{2\text{-loop}}}{\delta\mathbf{D}_{0\sigma,\pi}}\right)_{1\text{P I}}, \tag{46}$$

$$\Sigma=\left(\frac{\delta\ln Z_I^{2\text{-loop}}}{\delta\mathcal{D}_{0\psi}}\right)_{1\text{PI}}. \tag{47}$$

The self-energy graphs to each particle can be pictorially represented as by cutting one of the corresponding loops in the diagrams representing $(\ln Z_I^{2\text{-loop}})_{1\text{P I}}$. After the integration in x, τ and in the fields in $(\ln Z_I^{2\text{-loop}})_{1\text{PI}}$ and the differentiations above, we obtain the following expressions for the self-energies at one loop order:

$$\Pi_\pi(k_0,\mathbf{k})=\sum_{i=1}^{4}\Pi_{\pi i}=\lambda 5T\sum_n\int\frac{d^3p}{(2\pi)^3}\mathbf{D}_{0\pi}(\omega_n,\mathbf{p})+\lambda T\sum_n\int\frac{d^3p}{(2\pi)^3}\mathbf{D}_{0\sigma}(\omega_n,\mathbf{p})-4\lambda^2\nu^2T\sum_n\int\frac{d^3p}{(2\pi)^3}\mathbf{D}_{0\sigma}$$
$$\times(\omega_{n+l},\mathbf{p}+\mathbf{k})\mathbf{D}_{0\pi}(\omega_n,\mathbf{p})+g^2T\sum_n\int\frac{d^3p}{(2\pi)^3}\mathrm{Tr}[\gamma^5\mathcal{D}_{0\psi}(\omega_{n+l},\mathbf{p}+\mathbf{k})\gamma^5\mathcal{D}_{0\psi}(\omega_n,\mathbf{p})], \tag{48}$$

$$\Pi_\sigma(k_0,\mathbf{k})=\sum_{i=1}^{5}\Pi_{\sigma i}=3\lambda T\sum_n\int\frac{d^3p}{(2\pi)^3}\mathbf{D}_{0\sigma}(\omega_n,\mathbf{p})+3\lambda T\sum_n\int\frac{d^3p}{(2\pi)^3}\mathbf{D}_{0\pi}(\omega_n,\mathbf{p})-6\lambda^2\nu^2T\sum_n\int\frac{d^3p}{(2\pi)^3}\mathbf{D}_{0\pi}$$
$$\times(\omega_{n+l},\mathbf{p}+\mathbf{k})\mathbf{D}_{0\pi}(\omega_n,\mathbf{p})-18\lambda^2\nu^2T\sum_n\int\frac{d^3p}{(2\pi)^3}\mathbf{D}_{0\sigma}(\omega_{n+l},\mathbf{p}+\mathbf{k})\mathbf{D}_{0\sigma}(\omega_n,\mathbf{p})$$
$$+g^2T\sum_n\int\frac{d^3p}{(2\pi)^3}\mathrm{Tr}[\mathcal{D}_{0\psi}(\omega_{n+l},\mathbf{p}+\mathbf{k})\mathcal{D}_{0\psi}(\omega_n,\mathbf{p})], \tag{49}$$

$$\Sigma(k_0,\mathbf{k})=\sum_{i=1}^{2}\Sigma_i=-g^2T\sum_n\int\frac{d^3p}{(2\pi)^3}\mathbf{D}_{0\sigma}(\omega_{n+l},\mathbf{p}+\mathbf{k})\mathcal{D}_{0\psi}(\omega_n,\mathbf{p})-3g^2T\sum_n\int\frac{d^3p}{(2\pi)^3}\mathbf{D}_{0\pi}(\omega_{n+l},\mathbf{p}+\mathbf{k})\mathcal{D}_{0\psi}(\omega_n,\mathbf{p}). \tag{50}$$

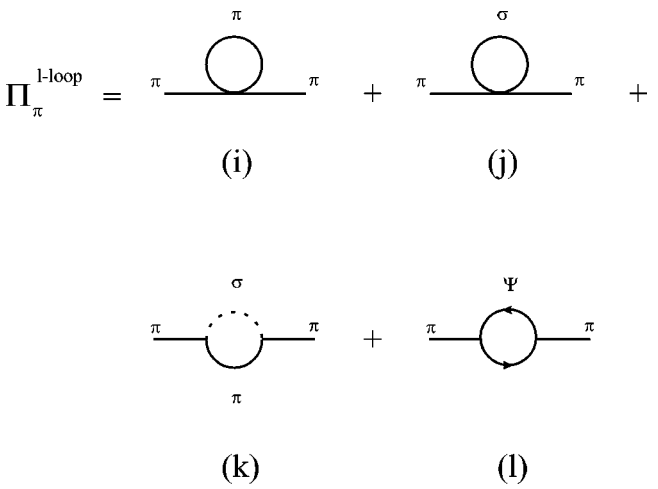

FIG. 2. One-loop self-energy for the pions.

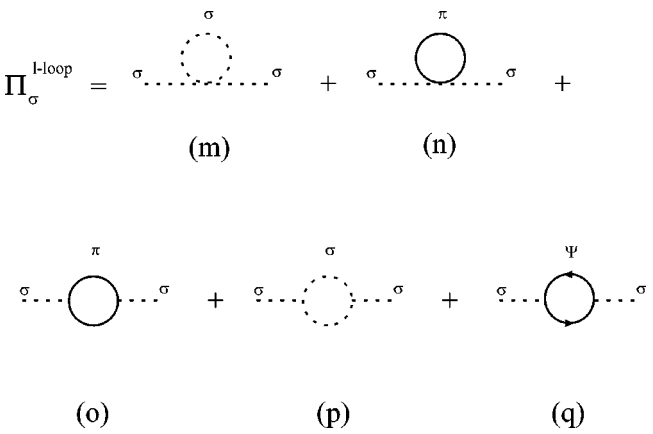

FIG. 3. One-loop self-energy for the meson sigma.

The diagrams representing the pion, sigma, and nucleon one-loop self-energies are drawn in Figs. 2, 3, and 4.

We note here that we could get the same results for the self-energies directly applying Feynman rules to construct the diagrams with the appropriate substitutions: the δ function at each vertex is replaced with a Kronecker delta which imposes conservation of the discrete energy ($k_0 = i\omega_n$), and round each loop of a thermal graph with $\int[d^4k/(2\pi)^4] \rightarrow (i/\beta)\Sigma_n \int[d^3k/(2\pi)^3]$,which are the finite-temperature Feynman rules [13,23]. When the summation over n is performed, each graph of the self-energies is separated into two parts, namely, a temperature independent part (at this stage), which is divergent, and a temperature dependent part containing the Bose-Einstein distribution in the case of bosons or the Fermi-Dirac distribution for fermions.

We will adopt the definition of mass at finite temperature as the real part of the pole of the corrected propagator at zero momentum ($\mathbf{k}=0$). Thus, from Eqs. (42) and (43) we have

$$\begin{aligned}\mathbf{D}_\pi(\omega_n,|\mathbf{k}|=0)^{-1} &= \omega_n^2 + m_\pi^2 + \Pi_\pi(\omega_n,|\mathbf{k}|=0) \\ &= 0 \rightarrow -k_{0,\pi}^2 + m_\pi^2 + \Pi_\pi(T,k_{0,\pi},|\mathbf{k}|=0) \\ &= 0, \end{aligned} \tag{51}$$

$$\begin{aligned}\mathbf{D}_\sigma(\omega_n,|\mathbf{k}|=0)^{-1} &= \omega_n^2 + m_\sigma^2 + \Pi_\sigma(\omega_n,|\mathbf{k}|=0) \\ &= 0 \rightarrow -k_{0,\sigma}^2 + m_\sigma^2 + \Pi_\sigma(T,k_{0,\sigma},|\mathbf{k}|=0) \\ &= 0, \end{aligned} \tag{52}$$

$$\begin{aligned}\mathcal{D}_\psi(\omega_n f,|\mathbf{k}|=0)^{-1} &= \gamma^\mu k_\mu - m_\psi + \Sigma_s + \gamma^\mu \Sigma_\mu \\ &= 0 \rightarrow k_{0,\psi} + \Sigma_0(T,k_{0,\psi},|\mathbf{k}|=0) \\ &\quad + \Sigma_s(T,k_{0,\psi}|\mathbf{k}|=0) - m_\psi \\ &= 0, \end{aligned} \tag{53}$$

where the arrow indicates an analytical continuation from discrete to continuous energies in Minkowski space. Hence the physical masses are the values of the $k_{0;\pi,\sigma,\psi}$ which are the zeros of the functions (51), (52), and (53) above, i.e., the location of the poles in the limit $\mathbf{k}=0$. The full self-energy expressions Π_π, Π_σ, Σ_0, and Σ_s are shown explicitly in Appendix B. The renormalization of the self-energy is studied in Sec. VI. Throughout this paper, we will use dimensional regularization, but omitting, for notational simplicity the factor $\mu^{2\epsilon}$ which multiplies λ. Since our calculation does not require traces involving an odd number of γ^5 matrices, we use the definition of γ^5 as in Refs. [24,25].

Since these expressions are self-consistent they have to be solved numerically. For each fixed temperature one finds a value of $M_{\pi,\sigma,\psi}$ which satisfies the equations above. On the other hand, if one is interested only in the meson sector of the linear sigma model, the integrals in the self-energies could be evaluated exactly in the high-temperature limit and at low frequency where the boson diagrams involving three-point vertices which are proportional to $\lambda^2\nu^2$ may be neglected. This is not consistent if one wants to study the behavior of the condensate ν and the particle masses in all ranges of temperatures. It is important to note that when $c=0$ the three-point vertex boson diagrams are significant in the region $T_i(\sim 0) < T < T_f[\sim \nu(T)]$ and when $c \neq 0$, $\nu(T) \neq 0$ for any finite value of T.

B. The second necessity: The resummation

The expressions for the self-energies appearing in Eqs. (51), (52), and (53) are functions of $\omega_{\pi,\sigma,\psi}$ which are expressed in terms of the mean-field masses. As we discussed, the meson masses become negative as the temperature increases. Thus, in the computation of the one-loop corrections, the masses running in the loops become tachyonic. A proper resummation of higher order loops is naturally necessary [6]. Various resummation methods have been proposed in a tentative of curing the problem of the breaking down of the perturbative expansion at high temperature. In effective models, when a phase transition occurs, one can find tachyonic masses even below T_c. The $O(N)$ linear σ model which is one of the laboratory effective models employed to study QCD has been investigated by different authors using different techniques. One of these methods is the Cornwall-

Jackiw-Tomboulis (CJT) formalism [26] which provides for a consistent loop expansion of the effective potential in terms of the full propagator. The CJT formalism elegantly provides for a gap equation from stationarity conditions for the daisy and superdaisy effective potential. However some authors use this nonperturbative approach with an ansatz for the full (corrected) propagator in which the thermal corrections are momentum independent. These corrections are the finite piece of the divergent integral (which is temperature dependent through the gap equation for M) plus the finite explicit temperature dependent piece. This is the Hartree approximation, and means resuming only the ''bubble diagrams'' that are dominant at high temperatures. Another nonperturbative approach widely found in the literature is the large-N approximation. The $N\rightarrow\infty$ limit facilitates the calculations, but can lead to inaccuracies [27,19]. One must be careful in taking the large-N limit since its truncation depends on the problem to be studied and the relevant value of N [27]. In this case the three-point vertex diagrams are omitted which in principle makes sense only in the $N\rightarrow\infty$ limit since these sunset diagrams are of order $1/N$. In these two kinds of treatment one cannot study the bosons interacting with fermions (with the interactions of the linear sigma model) since the self-energy diagrams are momentum dependent which invalidates the ansatz cited above. It is worth remembering that the Hartree approximation does not satisfy the Goldstone theorem [19,28]. This fact may be attributed to the non inclusion of these diagrams. Although the finite temperature mass in these approaches is the pole of the corrected propagator, it is not the true mass, since their $\Pi_{\pi,\sigma}$ are not the true one-loop self-energy functions (see discussion below). The corrections included only shift the masses. Once we are interested in the study of the masses behavior also in the range $0<T<T_c$ (if $c=0$) the three-particle vertex diagrams will not be neglected. The inclusion of these diagrams brings an additional complication since the self-energy now depends on the momentum.

C. A nonperturbative resummation method: The MSCR

Let us now introduce our procedure which resums higher loop diagrams in the mean-field (tree-level) propagators. The method consists in recalculating the self-energy, in steps, using in each step the masses obtained in the previous one such that $M_n^2=(A_n+1)M_{n-1}^2+\Pi(M_{n-1})$, where n is the order of the nonperturbative correction and A_n is the coefficient of the appropriate counterterm. With this procedure it is easier to identify and absorb the divergent parts of the self-energy in order to have finite gap equations. The goal is to make renormalization possible since the masses which multiply the divergences are necessarily the same as in counterterms.

Application of MSCR. Here we apply the MSCR in the study of the chiral fermion meson model at finite temperature. The analysis of the problem has to be done carefully which will be divided into three regions.

Region I: The low-temperature region. The first region is for $0\leqslant T<T^*$, where T^* is the temperature where $\nu(T^*)=f_\pi$. This implies that $m_\pi^2=0$ and consequently the appearance of infrared divergences in the self-energy.

Step 1. Start with the mean-field effective Lagrangian where the condensate and the masses are given by

$$\{F[\omega_{\pi,\sigma,\psi}(m_{\pi,\sigma,\psi;0}),T]+G[\omega_{\pi,\sigma,\psi}(m_{\pi,\sigma,\psi;0})] -\lambda(f_\pi^2-\nu^2)\}\nu-c=0, \tag{54}$$

$$M_{\pi,0}^2=m_\pi^2=m^2+\lambda\nu^2, \tag{55}$$

$$M_{\sigma,0}^2=m_\sigma^2=m^2+3\lambda\nu^2, \tag{56}$$

$$M_{\psi,0}=m_\psi=g\nu. \tag{57}$$

Step 2. Evaluate the one-loop self-energy corrections to these masses from the equations presented in Appendix B and define the condensate and the first order corrected masses as

$$\{F[\omega_{\pi,\sigma,\psi}(M_{\pi,\sigma,\psi,0}),T]+G[\omega_{\pi,\sigma,\psi}(M_{\pi,\sigma,\psi,0})] -\lambda(f_\pi^2-\nu^2)\}\nu-c=0, \tag{58}$$

$$\begin{aligned} M_{\pi,1}^2&=M_{\pi,0}^2+\Pi_\pi(M_{\pi,0}^2,M_{\sigma,0}^2,M_{\psi,0})\\ &=(A_1+E_1+1)m^2+(\overline{A}_1+E_1+1)\lambda\nu^2\\ &\quad+\Pi_\pi(M_{\pi,0}^2,M_{\sigma,0}^2,M_{\psi,0})\\ &=m^2+\lambda\nu^2+\Pi_\pi^{Ren}(M_{\pi,0}^2,M_{\sigma,0}^2,M_{\psi,0}), \end{aligned} \tag{59}$$

$$\begin{aligned} M_{\sigma,1}^2&=M_{\sigma,0}^2+\Pi_\sigma(M_{\pi,0}^2,M_{\sigma,0}^2,M_{\psi,0})\\ &=(B_1+F_1+1)m^2+(F_1+1)\lambda\nu^2\\ &\quad+(\overline{B}_1+1)2\lambda\nu^2+\Pi_\sigma(M_{\pi,0}^2,M_{\sigma,0}^2,M_{\psi,0})\\ &=m^2+3\lambda\nu^2+\Pi_\sigma^{Ren}(M_{\pi,0}^2,M_{\sigma,0}^2,M_{\psi,0}), \end{aligned} \tag{60}$$

$$\begin{aligned} M_{\psi,1}&=M_{\psi,0}-\Sigma(M_{\pi,0}^2,M_{\sigma,0}^2,M_{\psi,0})\\ &=(C_1+1)g\nu-\Sigma(M_{\pi,0}^2,M_{\sigma,0}^2,M_{\psi,0})\\ &=g\nu-\Sigma^{Ren}(M_{\pi,0}^2,M_{\sigma,0}^2,M_{\psi,0}), \end{aligned} \tag{61}$$

where $\Pi_{\pi,\sigma}=\Pi_{\pi,\sigma}(k_{0,\pi,\sigma}=M_{\pi,\sigma};\mathbf{k}=0)^0+\Pi_{\pi,\sigma}(T;k_{0,\pi,\sigma}=0;\mathbf{k}=0)^\beta$, A_1, $\overline{A}_1$, B_1, $\overline{B}_1$, C_1, E_1, and F_1 are the appropriate coefficients of the counterterms added to the mean-field effective Lagrangian needed to render the model finite up to this order, which are shown in Sec. VI. The requirement that $k_{0,\pi,\sigma}=0$ in $\Pi_{\pi,\sigma}^\beta$ excludes the possibility of tachyonic tree-level masses since thermal effects provides for the pion a nonzero width due to the Landau damping process. For the fermions we adopt the requirement that $\Sigma=\Sigma(k_{0,\psi}=M_\psi;\mathbf{k}=0)^0+\Sigma(T;k_{0,\psi}=0;\mathbf{k}=0)^\beta$ to prevent a similar consequence. The resummation has to be done

exactly to avoid this problem. In this range there is no necessity of resummation since the masses running in the loops are positive, i.e., $M^2_{\pi,0}>0$, $M^2_{\sigma,0}>0$, and $M_{\psi,0}>0$.

Renormalization. The renormalization is done normally since the masses multiplying the divergences are the same as in the counterterms. The coefficients of the counterterms are found in Sec. VI.

Goldstone's theorem. In the exact chiral limit ($c=0$) and low-temperature phase (where $\nu\neq 0$) from Eq. (51) at ($k_0\rightarrow 0,|\mathbf{k}|=0$), we have

$$
\begin{aligned}
M^2_{\pi,1} &= M^2_{\pi,0}+\Pi_\pi(k_0\rightarrow 0,|\mathbf{k}|=0)\\
&= m^2+\lambda\nu^2+\Pi^{\mathrm{Ren}}_\pi(k_0\rightarrow 0,|\mathbf{k}|=0)\\
&= -\left\{\frac{3\lambda}{(4\pi)^2}\left[M^2_{\pi,0}\ln\left(\frac{M^2_{\pi,0}}{e\mu^2}\right)+M^2_{\sigma,0}\ln\left(\frac{M^2_{\sigma,0}}{e\mu^2}\right)\right]-\frac{8g^2}{(4\pi)^2}M^2_{\psi,0}\ln\left(\frac{M^2_{\psi,0}}{e\mu^2}\right)\right.\\
&\quad\left.+\int_0^\infty\frac{dp\,p^2}{2\pi^2}\left[3\lambda\left(\frac{n_\sigma(M_{\sigma,0})}{\omega_\sigma(M_{\sigma,0})}+\frac{n_\pi(M_{\pi,0})}{\omega_\pi(M_{\pi,0})}\right)+8g^2\frac{n_\psi(M_{\psi,0})}{\omega_\psi(M_{\psi,0})}\right]\right\}+\frac{5\lambda}{(4\pi)^2}M^2_{\pi,0}\ln\left(\frac{M^2_{\pi,0}}{e\mu^2}\right)\\
&\quad+\frac{5\lambda}{2}\int_0^\infty\frac{dp\,p^2}{\pi^2}\frac{n_\pi}{\omega_\pi}+\frac{\lambda}{(4\pi)^2}M^2_{\sigma,0}\ln\left(\frac{M^2_{\sigma,0}}{e\mu^2}\right)+\frac{\lambda}{2}\int_0^\infty\frac{dp\,p^2}{\pi^2}\frac{n_\sigma}{\omega_\sigma}-4\frac{\lambda^2\nu^2}{(4\pi)^2}\frac{M^2_{\pi,0}\ln\left(\frac{M^2_{\pi,0}}{e\mu^2}\right)-M^2_{\sigma,0}\ln\left(\frac{M^2_{\sigma,0}}{e\mu^2}\right)}{M^2_{\sigma,0}-M^2_{\pi,0}}\\
&\quad-2\lambda^2\nu^2\int_0^\infty\frac{dp\,p^2}{\pi^2}\left[\frac{n_\pi}{\omega_\pi}\frac{1}{M^2_{\sigma,0}-M^2_{\pi,0}}-\frac{n_\sigma}{\omega_\sigma}\frac{1}{M^2_{\sigma,0}-M^2_{\pi,0}}\right]-\frac{8g^2}{(4\pi)^2}M^2_{\psi,0}\ln\left(\frac{M^2_{\psi,0}}{e\mu^2}\right)+4g^2\int_0^\infty\frac{dp\,p^2}{\pi^2}\frac{n_\psi}{\omega_\psi}\\
&= 0
\end{aligned}
\tag{62}
$$

since $M^2_{\sigma,0}-M^2_{\pi,0}=2\lambda\nu^2$ [in deriving Eq. (62) we have used Eq. (29)].

Region II: The intermediate temperature region. This is the region for $T^*\leqslant T\leqslant T_c$ where the resummation is really necessary, since the masses in the loops are zero or tachyonic. The problem here is more complicated than in the other temperature regions since phase transition takes place. As is well known, around the critical temperature quantum fluctuations become essential and one loop corrections may not be enough. In fact, as we proceed to show here, this scheme (i.e., allowing only one loop corrections in the perturbative expansion) prevents us from adequately renormalizing the gap equations for the tree-level resummed masses and satisfying Goldstone's theorem.

We show next that this is indeed the case and that a possible (but inconsistent) way of achieving renormalization, would be, e.g., to consider only the diagrams for which $\Pi_\pi=\Pi_\sigma$. This is very frequently implemented in the literature [12,18,19,28].

We will adopt the point of view that the MSCR fails in this region and higher order loop corrections in the perturbative expansion will be necessary at this stage. This is the subject of current investigation. However, we explicitly show where the problem appears.

Step 1. Start with the mean-field effective Lagrangian where the condensate and the masses are given by

$$
\begin{aligned}
&\{F[\omega_{\pi,\sigma,\psi}(m_{\pi,\sigma,\psi;0}),T]+G[\omega_{\pi,\sigma,\psi}(m_{\pi,\sigma,\psi;0})]\\
&\quad-\lambda(f_\pi^2-\nu^2)\}\nu-c=0,
\end{aligned}
\tag{63}
$$

$$
M^2_{\pi,0}=m^2_\pi=m^2+\lambda\nu^2, \tag{64}
$$

$$
M^2_{\sigma,0}=m^2_\sigma=m^2+3\lambda\nu^2, \tag{65}
$$

$$
M_{\psi,0}=m_\psi=g\nu. \tag{66}
$$

Step 2. Evaluate the one-loop self-energy corrections to these masses from the equations presented in Appendix B and define the condensate and the first order corrected masses as

$$
\begin{aligned}
&\{F[\omega_{\pi,\sigma,\psi}(M_{\pi,\sigma,\psi,0}),T]+G[\omega_{\pi,\sigma,\psi}(M_{\pi,\sigma,\psi,0})]\\
&\quad-\lambda(f_\pi^2-\nu^2)\}\nu-c=0,
\end{aligned}
\tag{67}
$$

$$M^2_{\pi,1}=M^2_{\pi,0}+\Pi_\pi(M^2_{\pi,0},M^2_{\sigma,0},M_{\psi,0})$$
$$=(A_1+E_1+1)m^2+(\overline{A}_1+E_1+1)\lambda\nu^2$$
$$+\Pi_\pi(M^2_{\pi,0},M^2_{\sigma,0},M_{\psi,0})$$
$$=m^2+\lambda\nu^2+\Pi^{\rm Ren}_\pi(M^2_{\pi,0},M^2_{\sigma,0},M_{\psi,0}), \quad (68)$$

$$M^2_{\sigma,1}=M^2_{\sigma,0}+\Pi_\sigma(M^2_{\pi,0},M^2_{\sigma,0},M_{\psi,0})$$
$$=(B_1+F_1+1)m^2+(F_1+1)\lambda\nu^2$$
$$+(\overline{B}_1+1)2\lambda\nu^2+\Pi_\sigma(M^2_{\pi,0},M^2_{\sigma,0},M_{\psi,0})$$
$$=m^2+3\lambda\nu^2+\Pi^{\rm Ren}_\sigma(M^2_{\pi,0},M^2_{\sigma,0},M_{\psi,0}), \quad (69)$$

$$M_{\psi,1}=M_{\psi,0}-\Sigma(M^2_{\pi,0},M^2_{\sigma,0},M_{\psi,0})$$
$$=(C_1+1)g\nu-\Sigma(M^2_{\pi,0},M^2_{\sigma,0},M_{\psi,0})$$
$$=g\nu-\Sigma^{\rm Ren}(M^2_{\pi,0},M^2_{\sigma,0},M_{\psi,0}). \quad (70)$$

At this stage of the application of the method, the renormalization is possible, Goldstone's theorem is verified, but the tree-level masses are zero or tachyonic.

Step 3. Now we take the masses computed in the previous step and improve the results defining a next-order nonperturbative correction. With this we get a new effective Lagrangian where the condensate and masses are given by

$$\{F[\omega_{\pi,\sigma,\psi}(M_{\pi,\sigma,\psi,1}),T]+G[\omega_{\pi,\sigma,\psi}(M_{\pi,\sigma,\psi,1})]$$
$$-\lambda(f_\pi^2-\nu^2)\}\nu-c=0, \quad (71)$$

$$M^2_{\pi,2}=M^2_{\pi,1}+\Pi_\pi(M^2_{\pi,1},M^2_{\sigma,1},M_{\psi,1})$$
$$=(A_2+E_2+1)m^2+(\overline{A}_2+E_2+1)\lambda\nu^2$$
$$+(\overline{\overline{A}}_2+E_2+1)\Pi^{\rm Ren}_\pi(M^2_{\pi,0},M^2_{\sigma,0},M_{\psi,0})$$
$$+\Pi_\pi(M^2_{\pi,1},M^2_{\sigma,1},M_{\psi,1})$$
$$=m^2+\lambda\nu^2+\Pi^{\rm Ren}_\pi(M^2_{\pi,1},M^2_{\sigma,1},M_{\psi,1})$$
$$-\frac{\lambda}{(4\pi)^2}\Pi^{\rm Ren}_\sigma(M^2_{\pi,1},M^2_{\sigma,1},M_{\psi,1})\frac{1}{\tilde{\epsilon}}, \quad (72)$$

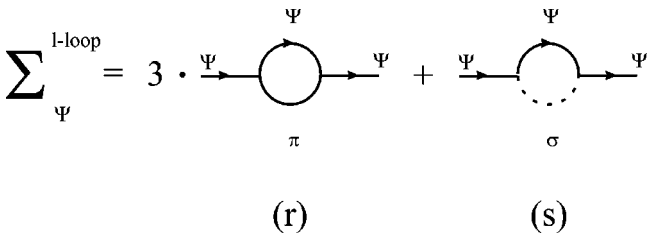

FIG. 4. One-loop self-energy for the fermions. Note that the lowest corrections for the fermions are of order g^2.

$$M^2_{\sigma,2}=M^2_{\sigma,1}+\Pi_\sigma(M^2_{\pi,1},M^2_{\sigma,1},M_{\psi,1})$$
$$=(B_2+F_2+1)m^2+(F_2+1)\lambda\nu^2$$
$$+(\overline{B}_2+1)2\lambda\nu^2+(\overline{\overline{B}}_2+F_2+1)$$
$$\times\Pi^{\rm Ren}_\sigma(M^2_{\pi,0},M^2_{\sigma,0},M_{\psi,0})$$
$$+\Pi_\sigma(M^2_{\pi,1},M^2_{\sigma,1},M_{\psi,1})$$
$$=m^2+3\lambda\nu^2+\Pi^{\rm Ren}_\sigma(M^2_{\pi,1},M^2_{\sigma,1},M_{\psi,1})$$
$$-\frac{3\lambda}{(4\pi)^2}\Pi^{\rm Ren}_\pi(M^2_{\pi,1},M^2_{\sigma,1},M_{\psi,1})\frac{1}{\tilde{\epsilon}}, \quad (73)$$

$$M_{\psi,2}=M_{\psi,1}-\Sigma(M^2_{\pi,1},M^2_{\sigma,1},M_{\psi,1})(C_2+1)g\nu$$
$$-(\overline{C}_2+1)\Sigma^{\rm Ren}(M^2_{\pi,0},M^2_{\sigma,0},M_{\psi,o})$$
$$-\Sigma(M^2_{\pi,1},M^2_{\sigma,1},M_{\psi,1})$$
$$=g\nu-\Sigma^{\rm Ren}(M^2_{\pi,1},M^2_{\sigma,1},M_{\psi,1}). \quad (74)$$

It is shown that in the $\lambda\phi^4$ model, this (first) recalculation is equivalent to the sum of an infinite set of diagrams, namely, the ''daisy'' sum [6] or the set of ring [13]. The coefficients of the temperature dependent mass counterterms $\overline{\overline{A}}_2$, $\overline{\overline{B}}_2$, and $\overline{C}_2$ are fixed in a manner to cancel not only divergences proportional to $\Pi^{\rm Ren}_\pi(M^2_{\pi,0},M^2_{\sigma,0},M_{\psi,0})$, $\Pi^{\rm Ren}_\sigma(M^2_{\pi,0},M^2_{\sigma,0},M_{\psi,0})$, and $\Sigma^{\rm Ren}(M^2_{\pi,0},M^2_{\sigma,0},M_{\psi,o})$, respectively, but also these terms together. That is, at each stage of the procedure, for $n>1$, in the expressions for $M_{\pi,\sigma,\psi,n}$, the self-energy $\Pi_{\pi,\sigma}(M_{\pi,\sigma,\psi,n-2})$ [or $\Sigma(M_{\pi,\sigma,\psi,n-2})$] have to be canceled to avoid overcounting of diagrams.

This shows explicitly that renormalization can not be performed within this approximation scheme. This is not surprising since in this temperature region quantum fluctuation may need a more thorough description. So, there is no reason to believe that only the ''daisy'' diagrams should be resummed at low and intermediate temperatures. In fact, the ''daisy'' graphs contributions are dominant at high temperature [6].

Renormalization. Since in this region $M^2_{\sigma,n}-M^2_{\pi,n}=2\lambda\nu^2+\Delta\Pi$, where $\Delta\Pi\equiv\Pi_\sigma-\Pi_\pi$, there is the presence of undesirable nonrenormalizable terms. These terms are the last ones on the right-hand side of Eqs. (72) and (73) which come from Eqs. (B2) and (B6), respectively, and cannot be absorbed in the counterterms.

Goldstone's theorem. In this region, Goldstone's theorem is satisfied only if $\Delta\Pi\to 0$ and the contribution in Eq. (B3) is decoupled into integrals proportional to λ. This would assure the cancellation of M_π at $(k_0\to 0,|\mathbf{k}|=0)$. The reason for this frustration is the same as for the lack of renormalizability.

Step 4. (Applicable only in the case where $\Delta\Pi=0$. This guarantees that renormalization and Goldstone theorem can be satisfactorily implemented at each step. In particular this will be the case for the high-temperature region as will be shown next.)

Proceeding with the iteration, in the limit $n\to\infty$ the masses M_n have formally the same expressions as the masses M_{n-1} which are already renormalized. Thus, in this limit we will have

$$\{F[\omega_{\pi,\sigma,\psi}(M_{\pi,\sigma,\psi,n}),T]+G[\omega_{\pi,\sigma,\psi}(M_{\pi,\sigma,\psi,n})] - \lambda(f_\pi^2-\nu^2)\}\nu-c=0, \tag{75}$$

$$M_{\pi,n}^2=m^2+\lambda\nu^2+\Pi_\pi^{\rm Ren}(M_{\pi,n}^2,M_{\sigma,n}^2,M_{\psi,n}), \tag{76}$$

$$M_{\sigma,n}^2=m^2+3\lambda\nu^2+\Pi_\pi^{\rm Ren}(M_{\pi,n}^2,M_{\sigma,n}^2,M_{\psi,n}), \tag{77}$$

$$M_{\psi,n}=g\nu-\Sigma^{\rm Ren}(M_{\pi,n}^2,M_{\sigma,n}^2,M_{\psi,n}). \tag{78}$$

At each intermediate step, in the loops we set $k_{0\pi,\psi}^2=M_{\pi,\psi,n-1}^2$ in the computation of $M_{\pi,\sigma,\psi,n}^2$. This ensures the cancellation of the divergences in all stages of the process, since the masses in the counterterms will necessarily be the same as in the divergences. In the end, in the resulting equations of interest (to be solved nummerically), $K_{0\pi,\psi}^2=M_{\pi,\psi}^2$ as it should. By our MSCR we have gotten a set of four coupled nonlinear integral equations to be solved self-consistently, with finite gap equations for the tree-level masses, which read

$$M_\pi^2=m^2+\lambda\nu^2+\Pi_\pi^{\rm Ren}(k_{0\pi}=M_\pi,|\mathbf{k}|=0), \tag{79}$$

$$M_\sigma^2=m^2+3\lambda\nu^2+\Pi_\pi^{\rm Ren}(k_{0\pi}=M_\pi,|\mathbf{k}|=0), \tag{80}$$

$$M_\psi=g\nu-\Sigma_0^{\rm Ren}(k_{0\psi}=M_\psi,|\mathbf{k}|=0) -\Sigma_s^{\rm Ren}(k_{0\psi}=M_\psi,|\mathbf{k}|=0), \tag{81}$$

$$\nu\left\{m^2+\lambda\nu^2+\frac{3\lambda}{(4\pi)^2}\left[M_\pi^2\ln\left(\frac{M_\pi^2}{e\mu^2}\right)+M_\sigma^2\ln\left(\frac{M_\sigma^2}{e\mu^2}\right)\right] -\frac{8g^2}{(4\pi)^2}M_\psi^2\ln\left(\frac{M_\psi^2}{e\mu^2}\right)+\int_0^\infty\frac{dp\,p^2}{2\pi^2}\left[3\lambda\left(\frac{n_\sigma(M_\sigma)}{\omega_\sigma(M_\sigma)} +\frac{n_\pi(M_\pi)}{\omega_\pi(M_\pi)}\right)+8g^2\frac{n_\psi(M_\psi)}{\omega_\psi(M_\psi)}\right]\right\}=c, \tag{82}$$

where the renormalization scale μ can be determined by a physical condition. We choose μ such that the pion mass has the correct value at $T=0$.

Now we have to go back to real world encoded by Eqs. (51)–(53). In order to get finite physical masses from the pole of these equations it is necessary to sum and subtract the finite quantities $\Pi_\pi^{\rm Ren}$ and $\Sigma^{\rm Ren}$ which will be regarded as mass parameters [7,10–12]. This corresponds to the reorganization of the perturbative expansion. Now we rewrite Eq. (20) as

$$\mathcal{L}=-\frac{\lambda}{4}(f_\pi^2-\nu^2)^2+c\nu+\overline{\psi}[i\gamma^\mu\partial_\mu-M_\psi]\psi +\frac{1}{2}[(\partial\vec{\pi})^2-M_\pi^2\vec{\pi}^2+(\partial\sigma)^2-M_\sigma^2\sigma^2] -g\overline{\psi}[\sigma+i\gamma^5\vec{\pi}\cdot\vec{\tau})]\psi-\frac{\lambda}{4}[(\vec{\pi}^2+\sigma^2)^2+4\nu\sigma(\vec{\pi}^2+\sigma^2)] +\Sigma^{\rm Ren}\overline{\psi}\psi+\frac{1}{2}\Pi_\pi^{\rm Ren}(\vec{\pi}^2+\sigma^2)+{\rm CT}. \tag{83}$$

The last two terms on the third line of Eq. (83) must be considered as extra ''interaction'' terms and will naturally be present in $\ln Z_I$, Eq. (41). The counterterm structure of Eq. (83) is the same as the one present in the method for the pion and fermion, differing only by numerical factors in the case of the sigma mass renormalization. By Eqs. (46) and (47) the extra contribution to the self-energy read

$$\Pi_\pi^{\rm extra}=\Pi_\sigma^{\rm extra}=-\Pi_\pi^{\rm Ren}, \tag{84}$$

$$\Sigma^{\rm extra}=\Sigma^{\rm Ren}, \tag{85}$$

where we have defined

$$\Pi_\pi^{\rm Ren}\equiv\Pi_\pi(k_{0,\pi}=M_\pi,\mathbf{k}=0)^0+\Pi_\pi(T,k_0=0,\mathbf{k}=0)^\beta, \tag{86}$$

$$\Sigma^{\rm Ren}\equiv\Sigma(k_0=M_\psi,\mathbf{k}=0)^0+\Sigma(T,k_0=0,\mathbf{k}=0)^\beta. \tag{87}$$

As a result, the final resummmed tree-level masses [Eqs. (79), (80), and (81)], may be used in Eqs. (51), (52), and (53) if one wants to study, for instance, spectral functions as the authors of Ref. [12], or decay width as in Ref. [28].

Goldstone's theorem. If the sunset type graphs are neglected, the self-energy function at one loop is not complete, despite the fact that the definition of masses as poles of propagators at zero momentum is still valid. Now, having the result for the full one-loop (and higher-order loops contributions from the resummation) self-energy function we can test algebraically the fulfillment of Goldstone's theorem in the exact chiral limit ($c=0$) and low-temperature phase (where $\nu\neq0$). From Eq. (51) at $(k_0\to0,|\mathbf{k}|=0)$, we have

$$
\begin{aligned}
M_\pi^2+\Pi_\pi^{\text{total}} &= M_\pi^2+\Pi_\pi(k_0\to 0,|\mathbf{k}|=0)+\Pi_\pi^{\text{extra}} \\
&= m^2+\lambda\nu^2+\Pi_\pi^{\text{Ren}}(k_0\to 0,|\mathbf{k}|=0) \\
&= -\left\{\frac{3\lambda}{(4\pi)^2}\left[M_\pi^2\ln\left(\frac{M_\pi^2}{e\mu^2}\right)+M_\sigma^2\ln\left(\frac{M_\sigma^2}{e\mu^2}\right)\right]-\frac{8g^2}{(4\pi)^2}M_\psi^2\ln\left(\frac{M_\psi^2}{e\mu^2}\right)+\int_0^\infty\frac{dp\,p^2}{2\pi^2}\right. \\
&\quad\left.\times\left[3\lambda\left(\frac{n_\sigma(M_\sigma)}{\omega_\sigma(M_\sigma)}+\frac{n_\pi(M_\pi)}{\omega_\pi(M_\pi)}\right)+8g^2\frac{n_\psi(M_\psi)}{\omega_\psi(M_\psi)}\right]\right\}+\frac{5\lambda}{(4\pi)^2}M_\pi^2\ln\left(\frac{M_\pi^2}{e\mu^2}\right)+\frac{5\lambda}{2}\int_0^\infty\frac{dpp^2}{\pi^2}\frac{n_\pi}{\omega_\pi} \\
&\quad+\frac{\lambda}{(4\pi)^2}M_\sigma^2\ln\left(\frac{M_\sigma^2}{e\mu^2}\right)+\frac{\lambda}{2}\int_0^\infty\frac{dp\,p^2}{\pi^2}\frac{n_\sigma}{\omega_\sigma}-4\frac{\lambda^2\nu^2}{(4\pi)^2}\frac{M_\pi^2\ln\left(\frac{M_\pi^2}{e\mu^2}\right)-M_\sigma^2\ln\left(\frac{M_\sigma^2}{e\mu^2}\right)}{M_\sigma^2-M_\pi^2} \\
&\quad-2\lambda^2\nu^2\int_0^\infty\frac{dp\,p^2}{\pi^2}\left[\frac{n_\pi}{\omega_\pi}\frac{1}{M_\sigma^2-M_\pi^2}-\frac{n_\sigma}{\omega_\sigma}\frac{1}{M_\sigma^2-M_\pi^2}\right]-\frac{8g^2}{(4\pi)^2}M_\psi^2\ln\left(\frac{M_\psi^2}{e\mu^2}\right)+4g^2\int_0^\infty\frac{dp\,p^2}{\pi^2}\frac{n_\psi}{\omega_\psi}=0
\end{aligned}
\tag{88}
$$

since $M_\sigma^2-M_\pi^2=2\lambda\nu^2$ [in deriving Eq. (88) we have used Eq. (82)].

In our opinion the satisfaction of Goldstone's theorem is ultimately related to the preservation of the relation imposed by chiral symmetry to the tree-level masses. Moreover, it is crucial to keep all diagrams of a given order. This is due to the fact that, strictly speaking, a loop expansion is an expansion in powers of the Lagrangian. As discussed in Ref. [13] in order to respect the symmetries of the Lagrangian, one must retain all diagrams to the given number of loops.

Then, in the absence of the explicit chiral symmetry breaking term, one has, for $0<T<T_c$,

$$
\begin{aligned}
M_\pi^2&=0, \\
M_\sigma^2&=2\lambda\nu^2,
\end{aligned}
\tag{89}
$$

for $T=T_c$,

$$
M_\pi^2=M_\sigma^2=0, \tag{90}
$$

and, for $T>T_c$,

$$
M_\pi^2=M_\sigma^2=m^2+3\lambda\int_0^\infty\frac{dp\,p^2}{\pi^2}\frac{n_b}{\omega_b}+4g^2\int_0^\infty\frac{dp\,p^2}{\pi^2}\frac{n_f}{\omega_f} \tag{91}
$$

which shows chiral symmetry restoration. Here *b* stands for bosons and *f* for fermions. We could interpret the result in the right-hand side of Eq. (91) as if each independent pion effectively ''sees'' one sigma and the other two pions and four fermions (since the chemical potential here is zero). On the other hand the sigma ''sees'' the three pions and four fermions. This equation serves to define the critical temperature in which the common masses of the particles vanish. In the high-temperature limit of these integrals, we find that $T_c^2=2f_\pi^2/(1+2g^2/3\lambda)$, as predicted by the mean-field analysis in Eq. (37).

Region III: The high-temperature region. This is the region of high temperatures $T\geqslant T_c$, if $c=0$ and $\nu=0$ or $T\geqslant T_i$, where T_i is defined as an ''inflexion'' temperature, for the case $c\neq 0$ and $\nu\ll f_\pi$ such that $M_{\pi,0}^2\approx M_{\sigma,0}^2=m^2$:

$$
\begin{aligned}
M_{\pi,1}^2&=M_{\pi,0}^2+\Pi_\pi(M_{\pi,0}^2,M_{\sigma,0}^2,M_{\psi,0}) \\
&=m^2+\Pi_\pi(M_{\pi,0}^2,M_{\sigma,0}^2,M_{\psi,0}),
\end{aligned}
\tag{92}
$$

$$
\begin{aligned}
M_{\sigma,1}^2&=M_{\sigma,0}^2+\Pi_\sigma(M_{\pi,0}^2,M_{\sigma,0}^2,M_{\psi,0}) \\
&=m^2+\Pi_\sigma(M_{\pi,0}^2,M_{\sigma,0}^2,M_{\psi,0}) \\
&=m^2+\Pi_\pi(M_{\pi,0}^2,M_{\sigma,0}^2,M_{\psi,0}) \\
&=M_{\pi,1}^2\equiv M_1^2,
\end{aligned}
\tag{93}
$$

$$
\begin{aligned}
M_{\psi,1}&=M_{\psi,0}-\Sigma(M_{\pi,0}^2,M_{\sigma,0}^2,M_{\psi,0}) \\
&=g\nu-\Sigma(M_{\pi,0}^2,M_{\sigma,0}^2,M_{\psi,0}).
\end{aligned}
\tag{94}
$$

Note that the pion and sigma masses become degenerate and the problem encountered in the previous region ($T^*\leqslant T\leqslant T_c$) is no longer here since $\Delta\Pi=0$ in this region of temperatures. In this case, the masses in the loops can be neglected, and we have

$$
\begin{aligned}
M_1^2=(A_1+1)M_0^2+\Pi(M_0)&=m^2+\frac{\lambda}{2}\left(1+\frac{2g^2}{3\lambda}\right)T^2 \\
&=\lambda f_\pi^2\left[\frac{T^2}{T_c^2}-1\right].
\end{aligned}
\tag{95}
$$

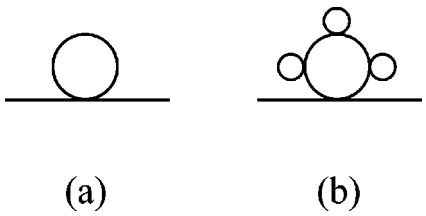

FIG. 5. (a) The 1PI one-loop self-energy diagram of the $\lambda\phi^4$ model and (b) a ''daisy'' type diagram with three attached bubbles which contributes to the self-energy.

If we set $g=0$ these results agree with the ones obtained by Bochkarev and Kapusta [22].

Following the iterations, we find for the nth iterated mass

$$M_n^2=(A_n+1)M_{n-1}^2+\Pi(M_{n-1})$$

$$=m^2+\frac{\lambda}{2}\left(1+\frac{2g^2}{3\lambda}\right)T^2\left[1-\frac{3}{\pi T}M_{n-1}\right]. \tag{96}$$

In the limit $n\to\infty$, we get

$$M^2=m^2+\frac{\lambda}{2}\left(1+\frac{2g^2}{3\lambda}\right)T^2\left[1-\frac{3}{\pi T}M\right], \tag{97}$$

which can be easily solved for M:

$$M=\left[\left(\frac{3\lambda f_\pi^2}{2\pi}\frac{T}{T_c^2}\right)^2+\lambda f_\pi^2\left(\frac{T^2}{T_c^2}-1\right)\right]^{1/2}-\frac{3\lambda f_\pi^2}{2\pi}\frac{T}{T_c^2}. \tag{98}$$

For $T\gg T_c$,

$$M^2=\frac{\lambda}{2}\left(1+\frac{2g^2}{3\lambda}\right)T^2. \tag{99}$$

V. THE MASSLESS $\lambda\phi^4$ AT HIGH TEMPERATURE

Now we apply the MSCR to study a very popular model: the massless $\lambda\phi^4$ model in the weak coupling limit

$$\mathcal{L}=\frac{1}{2}(\partial_\mu\phi)^2-\frac{\lambda}{4!}\phi^4, \tag{100}$$

$$M_0=0,$$

$$M_1^2=M_0^2+\Pi(M_0)=\frac{\lambda T^2}{24}, \tag{101}$$

and at this stage of the procedure there is no necessity of adding counterterms since up to this order there are no ultraviolet divergences in dimensional regularization [11]. Here Π is the 1PI one-loop self-energy to lowest order, namely, the ''bubble'' of Fig. 5(a):

$$M_2^2=M_1^2+\Pi(M_1)=(A_2+1)\Pi^{\mathrm{Ren}}(M_0)+\Pi(M_1)$$

$$=\frac{\lambda T^2}{24}\left(1-\frac{3M_1}{\pi T}\right)+O(\lambda^2\ln\lambda)$$

$$=M_1^2\left[1-3\left(\frac{\lambda}{24\pi^2}\right)^{1/2}\right]+O(\lambda^2\ln\lambda), \tag{102}$$

with the result that this correction to the mass is of order $\lambda^{3/2}$, which is a signature of the nonperturbative resummation. The temperature dependent counterterm is fixed so as to cancel the divergence and avoid overcounting of diagrams, as explained before. So, $A_2=-1+[\lambda/2(4\pi)^2](1/\epsilon)$. The diagrams used, in a given number of loops, in any resummation method must be the same in all stages of the process. What changes is the masses running in the loops at each iteration. This is because one must keep the same fundamental theory in the recalculation of the self-energy. The result shown in Eq. (102) is in agreement with the one obtained by Parwani's resummed perturbative expansion [11] [see Eq. (2.12) of his paper]. The second iteration corrected mass M_2, which was obtained in our method evaluating Fig. 5(a) with M_1 in that loop can equivalently be achieved calculating the ''daisy'' sum, that is a summation of the infinite set of ''daisy'' diagrams of Fig. 5(b) with M_0 in the loops. In this case all ''daisy'' types diagrams are IR divergent since $M_0=0$, but their sum is IR finite [13,11].

Continuing the iterations, we find for the next correction

$$M_3^2=M_2^2+\Pi(M_2)$$

$$=\frac{\lambda T^2}{24}\left[1-\frac{3M_1}{\pi T}\left(1-\frac{3M_1}{\pi T}\right)^{1/2}\right]. \tag{103}$$

When $\lambda\ll 1$ we get

$$M_3^2=\frac{\lambda T^2}{24}\left[1-3\left(\frac{\lambda}{24\pi^2}\right)^{1/2}+\frac{9}{2}\left(\frac{\lambda}{24\pi^2}\right)\right] \tag{104}$$

and for the nth iteration, we obtain

$$M_n^2=\frac{\lambda T^2}{24}\left\{1+\sum_{j=1}^{n}\frac{1}{2^{j-1}}\left[-3\left(\frac{\lambda}{24\pi^2}\right)^{1/2}\right]^j\right\}. \tag{105}$$

The ''superdaisy'' sum [6] corresponds to the limit $n\to\infty$ of Eq. (105) and it can be summed up (for $\lambda\ll 1$) to give

$$M^2=\frac{\lambda T^2}{24}\left[\frac{1-\frac{3}{2}\left(\frac{\lambda}{24\pi^2}\right)^{1/2}}{1+\frac{3}{2}\left(\frac{\lambda}{24\pi^2}\right)^{1/2}}\right]. \tag{106}$$

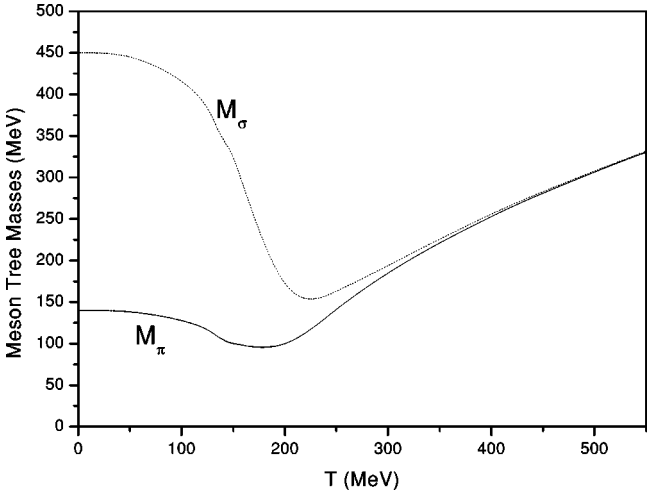

FIG. 6. Tree-level resumed meson masses.

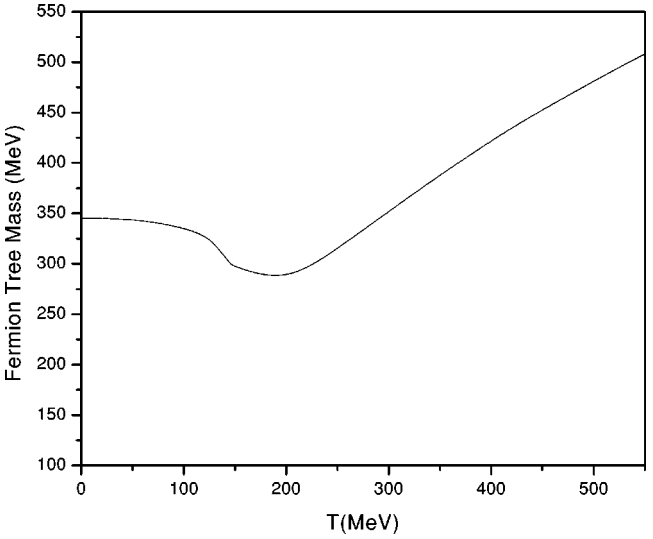

FIG. 7. Tree-level resumed fermion mass.

VI. RENORMALIZATION

A. Determination of the counterterms

The divergences are regulated via dimensional regularization. To renormalize the divergences, we use the minimal subtraction scheme where only the poles are eliminated by the appropriate counterterms. The first-order parameters of the temperature-dependent counterterms read

$$A_1=\frac{6\lambda}{(4\pi)^2}\frac{1}{\tilde{\epsilon}},\quad \overline{A}_1=\frac{12\lambda}{(4\pi)^2}\frac{1}{\tilde{\epsilon}},\quad E_1=\frac{4g^2}{(4\pi)^2}\frac{1}{\tilde{\epsilon}},\tag{107}$$

with $1/\tilde{\epsilon}\equiv 2/(4-d)-\gamma+\log(4\pi)$, where γ is the Euler constant,

$$B_1=\frac{6\lambda}{(4\pi)^2}\frac{1}{\tilde{\epsilon}},\quad \overline{B}_1=\frac{6\lambda}{(4\pi)^2}\frac{1}{\tilde{\epsilon}},\quad F_1=\frac{4g^2}{(4\pi)^2}\frac{1}{\tilde{\epsilon}},\tag{108}$$

$$C_1=\frac{8g^2}{(4\pi)^2}\frac{1}{\tilde{\epsilon}},\tag{109}$$

$$D_{1,1}=-8\left[\frac{1}{64\pi^2}\frac{1}{\tilde{\epsilon}}\right],\quad D_{2,1}=3\left[\frac{1}{64\pi^2}\frac{1}{\tilde{\epsilon}}\right],$$

$$D_{3,1}=\frac{1}{64\pi^2}\frac{1}{\tilde{\epsilon}}.\tag{110}$$

For all steps we always have

$$A_n=A_1,\overline{A}_n=\overline{A}_1,E_n=E_1,B_n=B_1,\overline{B}_n=\overline{B}_1,F_n=F_1,C_n=C_1,D_{1,2,3,n}=D_{1,2,3,1},\tag{111}$$

and for $n>1$,

$$\overline{\overline{A}}_n=-1+A_1,\overline{\overline{B}}_n=-1+B_1,\overline{\overline{C}}_n=-1-C_1.\tag{112}$$

B. Comments related with the presence of the fermions in the game

We must remark that, on Eqs. (B4), (B9), and (B10) of Appendix B, the following terms:

$$\frac{8g^2}{(4\pi)^2}m_\psi^2\frac{1}{\tilde{\epsilon}},\quad -\frac{8g^2}{(4\pi)^2}3m_\psi^2\frac{1}{\tilde{\epsilon}},$$

$$-\frac{g^2}{(4\pi)^2}\left[\frac{m_\sigma^2}{2k_0}\right]\frac{1}{\tilde{\epsilon}},\quad \text{and}\quad -\frac{g^2}{(4\pi)^2}\left[3\frac{m_\pi^2}{2k_0}\right]\frac{1}{\tilde{\epsilon}}$$

should be neglected. As stated by the authors of Ref. [29] and remarked by the authors of Ref. [12], these terms will be canceled by contributions from higher order loops. Since we are concerned only about the one-loop approximation, we do not have to worry about them. Nevertheless, in the $O(4)$ linear sigma model, i.e., when $g=0$, none of the above terms will be present, and our model will be order by order renormalizable in the regions of validity of the MSCR. This occurs because our tree-level resummed masses are related by a symmetry relation that always guarantees the cancellation of the UV divergences.

VII. NUMERICAL ANALYSIS

In this section, we present numerical solutions of the gap equations for the tree-level meson and fermion masses and the condensate derived in Sec. IV C including all diagrams which belong to the one loop order.

As an approximation, only for the sake of obtaining continuous curves, in the numerical evaluation we considered $\Delta\Pi=0$ also in the intermediate temperature region. Rigorously speaking, the curves should only be trusted in the low and high temperature regions. Figure 6 shows the tree-level resummed meson masses, Eqs. (79) and (80), as functions of the temperature. We show in Fig. 7 the tree-level fermion resummed mass, Eq. (81), as a function of temperature. The tree-level masses behavior exhibit the fact that the MSCR

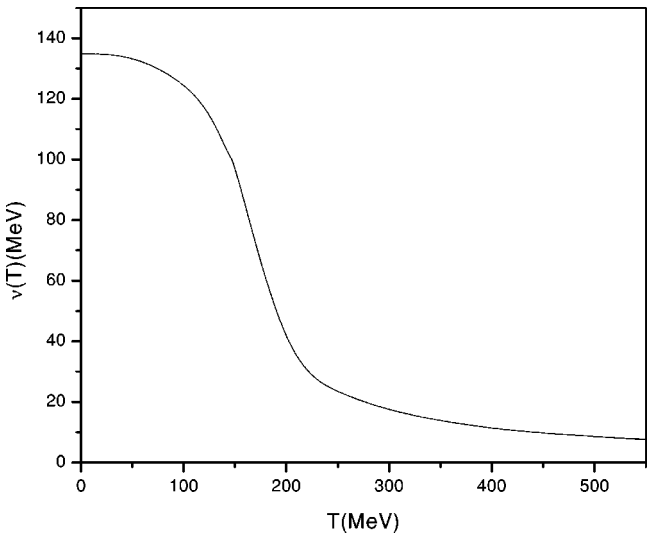

FIG. 8. Condensate ν as a function of the temperature.

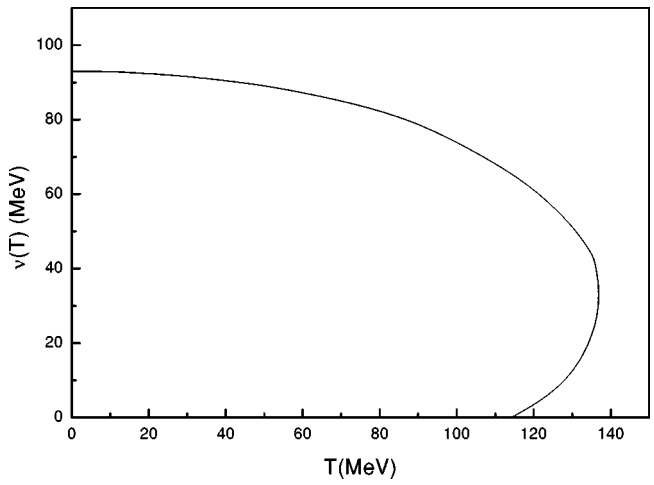

FIG. 9. Condensate ν as a function of the temperature in the chiral limit ($M_\pi = 0$).

has solved the problem of tachyonic masses. In Fig. 8 the chiral condensate ν, Eq. (82), as a function of temperature is shown whereas in Fig. 9 the condensate is plotted in the case $M_\pi = 0$.

Since at low temperatures the condensate dominates, the mesons masses suffers its influence in this region. The sigma mass decreases and they approach each other to become degenerate in a temperature of about 300 MeV. This confirms the results we found in a phenomenological approach to the linear sigma model [30].

The condensate is a slowly decreasing function of the temperature, which is a signature of the order parameter when the symmetry breaking term is present. The qualitative behavior of the results shown in Figs. 6 and 8 can be compared with the ones obtained by Chiku and Hatsuda [12] since OPT also sums three-point vertex diagrams, as our method does. Some differences may be attributed to the incorporation of the fermions, as performed in our method. In the absence of the chiral symmetry breaking term, i.e., when $c = 0$, the nonvanishing solutions of the extremum condition, Eq. (28), are obtained numerically by Eq. (82) with $M_\pi^2 = 0$, $M_\sigma^2 = 2\lambda\nu^2$, and $M_\psi = M_\psi(M_\pi^2 = 0, M_\sigma^2 = 2\lambda\nu^2)$. The solution is depicted in Fig. 9 and gives an indication of first order phase transition. This result agrees with the predictions of first order phase transition found in previous analysis by Roh and Matsui [18], Petropoulos [19], Chiku and Hatsuda [12], Randrup [31], and Bilic [32]. Of course we have to bear in mind that our result is at one loop order in the perturbative expansion. It may well be that near the critical temperature higher order corrections become crucial and may change the order of the phase transition.

The tree fermion mass, Fig. 7, does not become zero when chiral symmetry is restored and $\nu \to 0$ since we considered contributions from the mesons, given by Eq. (50). On the contrary, when the temperature is $\geqslant 200$ MeV these contributions dominate the variable ν and the fermion mass increases with temperature. The behavior of the fermion mass is in agreement with the results found by Panda in Ref. [33] for the quark meson coupling model.

VIII. CONCLUDING REMARKS

In this paper, we presented a modified self-consistent resummation (MSCR) at finite temperature. Results for the chiral fermion meson model and the massless $\lambda\phi^4$ model in the weak coupling limit were obtained and analyzed. We have shown that our procedure properly resumes higher order terms which cures the problem of the breakdown of the perturbative expansion.

We have also shown that the MSCR, when applied to the study of the chiral fermion meson model, has the essential features which lead to the satisfaction of Goldstone's theorem and renormalization of the UV divergences, in the low- and high-temperature regions. We have explicitly shown that the scheme breaks down around T_c, i.e., in the region of intermediate temperatures. The application of the MSCR in these three physically different regions (low, intermediate, and high temperatures) revealed a source of mistakes usually found in the literature, that is to treat all ranges of temperatures in the same way. It is naive to expect that the same approximation which is valid, e.g., for high temperatures would be enough in the intermediate-temperature region, since quantum fluctuations are known to play a major role there.

This division was essential to identify the regions where higher order terms and resummation are crucial. It is valid to remember that even when higher order loops are taken into account, the resummation is still necessary since the tree-level masses will become tachyonic even below the critical temperature (in theories with spontaneous symmetry breaking) and break the perturbative expansion. This breakdown of the perturbative expansion can also happen in massless field theories, such as QCD, due to the appearance of infrared divergences. As we discussed, the breakdown of perturbative expansion in finite temperature field theory requires resummation techniques as the MSCR to recover the reliability of perturbative expansion.

In each region renormalization and satisfaction of Goldstone's theorem were discussed in detail. In our study, we have also addressed a usually avoided point: the inclusion of

the fermions. Finally, we have reexamined the chiral phase transition in static equilibrium in terms of the linear sigma model with our MSCR.

The gap equations for the tree-level masses are constructed by our method and in the effective Lagrangian they are renormalized. For the particular case of intermediate-temperature regions, the gap equations would be renormalized in the (reorganized) effective Lagrangian only if $\Delta\Pi = \Pi_\sigma - \Pi_\pi = 0$. In most of the approximations found in the literature, the gap equations are reached by some technique or via some *ad hoc* procedure but the Lagrangian is yet the original one. This makes the renormalization process nontrivial, unless a finite cutoff is used and the theory is treated as an effective model [27,28]. As pointed out by Chiku and Hatsuda [12], the resummation must be done also in the counterterms, which is essential to show the renormalization.

At this point, it is extremely worth emphasizing that, although one has the freedom of adding and subtracting mass parameters to the Lagrangian, in this case they cannot be completely arbitrary. If the mass parameters introduced were different for the pion and sigma fields (i.e., $\frac{1}{2}M_1\sigma^2 + \frac{1}{2}M_2\vec{\pi}^2$ and, of course, the same quantities subtracted, with $M_1 \neq M_2$), neither the $O(4)$ linear σ model is renormalizable in any given order nor Goldstone's theorem is satisfied. This will happen even if the mass parameters are determined by some physical condition as FAC or principle of minimal sensitivity (PMS). So, the most important fact behind the fulfillment of Goldstone's theorem and renormalizability of theories with SSB is the chiral symmetry that must dictate which mass parameter should be introduced to the Lagrangian.

ACKNOWLEDGMENTS

One of the authors (H.C.G.C.) thanks the hospitality given by the Nuclear Theory group during his visit at the University of Minnesota where part of this work was done. He is gratefully indebted to Professors J. I. Kapusta and P. J. Ellis for various helpful advices and enlightening discussions. He is also grateful to Dr. M. Hott for valuable conversations about this problem, Professor A. Das for comments concerning the effective potential, and finally Drs. J. Lenaghan and S. Chiku for useful *e*-conversations. The authors would like to thank B. Hiller and A. Blin for useful comments on the subject of the paper. H.C.G.C. thanks the generous support provided by the Faculty of UFMG and FUNREI.

APPENDIX A: RENORMALIZATION OF THE EFFECTIVE POTENTIAL

As mentioned earlier the vacuum contribution to $\Omega_1(T,\nu)$ is divergent and requires renormalization. In this subsection we also use dimensional regularization in the computation of the effective potential:

$$\Omega_1^0(m) \equiv \int \frac{d^3p}{(2\pi)^3}\frac{\omega}{2}, \tag{A1}$$

$$\frac{\partial\Omega_1^0(m)}{\partial m} = m\int \frac{d^3p}{(2\pi)^3}\frac{1}{2\omega} = mL(m), \tag{A2}$$

where $L(m)$ is the usual zero-temperature loop integral,

$$L(m) \equiv \int \frac{d^4p}{(2\pi)^4}\frac{1}{p^2+m^2} = \int \frac{d^4p}{(2\pi)^4}\frac{1}{p_4^2+\mathbf{p}^2+m^2}, \tag{A3}$$

with $d^4p = dp_4\, d^3p$ being the four Euclidean momentum.

The divergent integral $L(m)$ can be evaluated in the standard manner

$$\frac{m^2}{(4\pi)^2}\left[-\frac{1}{\tilde{\epsilon}} - 1 + \ln\left(\frac{m^2}{\mu^2}\right)\right]. \tag{A4}$$

The quantity $\Omega_1^0(m)$ is then obtained with the integration of $mL(m)$

$$\Omega_1^0(m) = \frac{m^4}{64\pi^2}\left(\ln\frac{m^2}{\mu^2} - \frac{3}{2} - \frac{1}{\tilde{\epsilon}}\right). \tag{A5}$$

With this expression we can find the zero-temperature effective potential

$$\Omega_1^0(\nu) = -\frac{m_\sigma^4}{64\pi^2}\frac{1}{\tilde{\epsilon}} + \frac{m_\sigma^4}{64\pi^2}\left(\ln\frac{m_\sigma^2}{\mu^2} - \frac{3}{2}\right) + 3(m_\sigma \leftrightarrow m_\pi) - 8(m_\sigma \leftrightarrow m_\psi). \tag{A6}$$

The renormalization of the thermodynamical potential at the end amounts to the determination of the parameters $D_{1,2,3}$,

$$D_1 = -8\left[\frac{1}{64\pi^2}\frac{1}{\tilde{\epsilon}}\right], \tag{A7}$$

$$D_2 = 3\left[\frac{1}{64\pi^2}\frac{1}{\tilde{\epsilon}}\right], \tag{A8}$$

$$D_3 = \frac{1}{64\pi^2}\frac{1}{\tilde{\epsilon}}. \tag{A9}$$

APPENDIX B: ONE-LOOP SELF-ENERGY AT FINITE TEMPERATURE

At zero momentum the expressions for the self-energies are given by

$$\Pi_{\pi 1}(k_0, |\mathbf{k}| = 0) = \Pi_{\pi 1}^0 + \Pi_{\pi 1}^\beta = \frac{5\lambda}{(4\pi)^2}m_\pi^2\left[-\frac{1}{\tilde{\epsilon}} - 1 + \ln\left(\frac{m_\pi^2}{\mu^2}\right)\right] + \frac{5\lambda}{2}\int_0^\infty \frac{dp\, p^2}{\pi^2}\frac{n_\pi}{\omega_\pi}, \tag{B1}$$

$$\Pi_{\pi 2}(k_0,|\mathbf{k}|=0)=\Pi^0_{\pi 2}+\Pi^\beta_{\pi 2}$$
$$=\frac{\lambda}{(4\pi)^2}m_\sigma^2\left[-\frac{1}{\tilde{\epsilon}}-1+\ln\left(\frac{m_\sigma^2}{\mu^2}\right)\right]$$
$$+\frac{\lambda}{2}\int_0^\infty\frac{dp\,p^2}{\pi^2}\frac{n_\sigma}{\omega_\sigma}, \tag{B2}$$

$$\Pi_{\pi 3}(k_0,|\mathbf{k}|=0)$$
$$=\Pi^0_{\pi 3}+\Pi^\beta_{\pi 3}$$
$$=\frac{4\lambda^2\nu^2}{(4\pi)^2}\left[-\frac{1}{\tilde{\epsilon}}-1+\ln\left(\frac{m_\pi^2}{\mu^2}\right)+\frac{k_0^2+m_\sigma^2-m_\pi^2}{2k_0^2}\right.$$
$$\left.\times\ln\left(\frac{m_\pi^2}{m_\sigma^2}\right)+\frac{\sqrt{\Delta_3}}{k_0^2}(\Delta_4+\Delta_5)\right]-2\lambda^2\nu^2\int_0^\infty\frac{dpp^2}{\pi^2}$$
$$\times\left[\frac{n_\pi}{\omega_\pi}\frac{-k_0^2+m_\sigma^2-m_\pi^2}{(-k_0^2+m_\sigma^2-m_\pi^2)^2-2k_0^2(\omega_\pi^2+\omega_\sigma^2)}\right.$$
$$\left.+\frac{n_\sigma}{\omega_\sigma}\frac{-k_0^2+m_\pi^2-m_\sigma^2}{(-k_0^2+m_\pi^2-m_\sigma^2)^2-2k_0^2(\omega_\pi^2+\omega_\sigma^2)}\right], \tag{B3}$$

$$\Pi_{\pi 4}(k_0,|\mathbf{k}|=0)=\Pi^0_{\pi 4}+\Pi^\beta_{\pi 4}$$
$$=\frac{8g^2}{(4\pi)^2}\left[m_\psi^2-\frac{k_0^2}{2}\right]\frac{1}{\tilde{\epsilon}}+\frac{8g^2}{(4\pi)^2}$$
$$\times\left[-\left(m_\psi^2-\frac{k_0^2}{2}\right)\ln\left(\frac{m_\psi^2}{\mu^2}\right)+\Delta_2\sqrt{\Delta_1}-K_0^2\right]$$
$$+4g^2\int_0^\infty\frac{dpp^2}{\pi^2}\frac{n_\psi}{\omega_\psi}\left[1+\frac{k_0^2}{4\omega_{\psi^2}-k_0^2}\right], \tag{B4}$$

$$\Pi_{\sigma 1}(k_0,|\mathbf{k}|=0)=\Pi^0_{\sigma 1}+\Pi^\beta_{\sigma 1}$$
$$=\frac{3\lambda}{(4\pi)^2}m_\sigma^2\left[-\frac{1}{\tilde{\epsilon}}-1+\ln\left(\frac{m_\sigma^2}{\mu^2}\right)\right]$$
$$+\frac{3\lambda}{2}\int_0^\infty\frac{dpp^2}{\pi^2}\frac{n_\sigma}{\omega_\sigma}, \tag{B5}$$

$$\Pi_{\sigma 2}(k_0,|\mathbf{k}|=0)=\Pi^0_{\sigma 2}+\Pi^\beta_{\sigma 2}$$
$$=\frac{3\lambda}{(4\pi)^2}m_\pi^2\left[-\frac{1}{\tilde{\epsilon}}-1+\ln\left(\frac{m_\pi^2}{\mu^2}\right)\right]$$
$$+\frac{3\lambda}{2}\int_0^\infty\frac{dp\,p^2}{\pi^2}\frac{n_\pi}{\omega_\pi}, \tag{B6}$$

$$\Pi_{\sigma 3}(k_0,|\mathbf{k}|=0)=\Pi^0_{\sigma 3}+\Pi^\beta_{\sigma 3}$$
$$=18\frac{\lambda^2\nu^2}{(4\pi)^2}\left[-\frac{1}{\tilde{\epsilon}}-2+\ln\left(\frac{m_\sigma^2}{\mu^2}\right)\right.$$
$$\left.+2f_1(k_0)\arctan\left(\frac{1}{f_1(k_0)}\right)\right]$$
$$-18\lambda^2\nu^2\int_0^\infty\frac{dp^2}{\pi^2}\frac{n_\sigma}{\omega_\sigma}\frac{1}{4\omega_\sigma^2-k_0^2}, \tag{B7}$$

$$\Pi_{\sigma 4}(k_0,|\mathbf{k}|=0)=\Pi^0_{\sigma 4}+\Pi^\beta_{\sigma 4}$$
$$=6\frac{\lambda^2\nu^2}{(4\pi)^2}\left[-\frac{1}{\tilde{\epsilon}}-2+\ln\left(\frac{m_\pi^2}{\mu^2}\right)\right.$$
$$\left.+2f_2(k_0)\arctan\left(\frac{1}{f_2(k_0)}\right)\right]$$
$$-6\lambda^2\nu^2\int_{0\,T}^\infty\frac{dp\,p^2}{\pi^2}\frac{n_\pi}{\omega_\pi}\frac{1}{4\omega_\pi^2-k_0^2}, \tag{B8}$$

$$\Pi_{\sigma 5}(k_0,|\mathbf{k}|=0)$$
$$=\Pi^0_{\sigma 5}+\Pi^\beta_{\sigma 5}$$
$$=-\frac{8g^2}{(4\pi)^2}\left[3m_\psi^2-\frac{k_0^2}{2}\right]\frac{1}{\tilde{\epsilon}}+\frac{8g^2}{(4\pi)^2}$$
$$\times\left[\frac{1}{2}(6m_\psi^2-k_0^2)\ln\left(\frac{m_\psi^2}{\mu^2}\right)+(4m_\psi^2-k_0^2)\right.$$
$$\left.\times\left(\frac{\Delta_2\sqrt{\Delta_1}}{k_0^2}-1\right)\right]+4g^2\int_0^\infty\frac{dp\,p^2}{\pi^2}\frac{n_\psi}{\omega_\psi}$$
$$\times\left[1+\frac{4m_{\psi^2}-k_0^2}{k_0^2-4\omega_{\psi^2}}\right], \tag{B9}$$

where $f_1(k_0)=\sqrt{4m_\sigma^2/k_0^2-1}$, $f_2(k_0)=\sqrt{4m_\pi^2/k_0^2-1}$, $\Delta_1=k_0^2(k_0^2-4m_\psi^2)$, $\Delta_2=\arctan(1/\sqrt{1-4m_\psi^2/k_0^2})$, $\Delta_3=k_0^4-2k_0^2(m_\pi^2+m_\sigma^2)+(m_\pi^2-m_\sigma^2)^2$, $\Delta_4=\operatorname{arctanh}\{[k_0^2+(m_\pi^2+m_\sigma^2)]/\sqrt{\Delta_3}\}$ and $\Delta_5=\operatorname{arctanh}\{[k_0^2-(m_\pi^2+m_\sigma^2)]/\sqrt{\Delta_3}\}$,

$$
\begin{aligned}
&\Sigma(k_0,|\mathbf{k}|=0)\\
&\quad=(\Sigma_0+\Sigma_s)_\sigma+3(\Sigma_0+\Sigma_s)_\pi\\
&\quad=(\Sigma_0^0+\Sigma_0^\beta+\Sigma_s^0+\Sigma_s^\beta)_\sigma+3(\Sigma_0^0+\Sigma_0^\beta+\Sigma_s^0+\Sigma_s^\beta)_\pi\\
&\quad=\frac{g^2}{(4\pi)^2}\left[m_\psi+\frac{1}{2k_0}(k_0^2+m_\psi^2-m_\sigma^2)\right]\frac{1}{\tilde{\epsilon}}-\frac{g^2}{(4\pi)^2}m_\psi\left[\ln\left(\frac{m_\psi^2}{\mu^2}\right)+Z\right]-\frac{1}{(4\pi)^2}\frac{g^2}{2k_0}(k_0^2+m_\psi^2-m_\sigma^2)\left[\ln\left(\frac{m_\psi^2}{\mu^2}\right)+Z\right]\\
&\quad+\frac{g^2}{2}\int_0^\infty\frac{dp\,p^2}{\pi^2}\frac{n_\sigma}{\omega_\sigma}\frac{[k_0(-k_0^2+\omega_\sigma^2+\omega_\psi^2)+m_\psi(-k_0^2-\omega_\sigma^2+\omega_\psi^2)]}{[k_0^2-(\omega_\psi-\omega_\sigma)^2][k_0^2-(\omega_\psi+\omega_\sigma)^2]}+\frac{g^2}{2}\int_0^\infty\frac{dp\,p^2}{\pi^2}\frac{n_\psi}{\omega_\psi}\\
&\quad\times\frac{[2k_0\omega_\psi^2+m_\psi(k_0^2-\omega_\sigma^2+\omega_\psi^2)]}{[k_0^2-(\omega_\psi-\omega_\sigma)^2][k_0^2-(\omega_\psi+\omega_\sigma)^2]}+3(m_\sigma\leftrightarrow m_\pi),
\end{aligned}
\tag{B10}
$$

where $\Sigma_s(T,k_0,|\mathbf{k}|=0)$ is the scalar contribution, proportional to the unit matrix and $\Sigma_0(T,k_0,|\mathbf{k}|=0)$ is the contribution proportional to the matrix γ^0, and

$$
\begin{aligned}
(\Sigma_s^\beta)_\sigma&=\frac{g^2m_\psi}{2\pi^2}\int_0^\infty dp\,p^2\\
&\quad\times\left[\frac{n_\sigma}{\omega_\sigma}\frac{m_\psi^2-m_\sigma^2-k_0^2}{[k_0^2-(\omega_\psi-\omega_\sigma)^2][k_0^2-(\omega_\psi+\omega_\sigma)^2]}\right.\\
&\quad\left.+\frac{n_\psi}{\omega_\psi}\frac{m_\psi^2-m_\sigma^2+k_0^2}{[k_0^2-(\omega_\psi-\omega_\sigma)^2][k_0^2-(\omega_\psi+\omega_\sigma)^2]}\right],
\end{aligned}
\tag{B11}
$$

$$
\begin{aligned}
(\Sigma_0^\beta)_\sigma&=\frac{g^2k_0}{2\pi^2}\int_0^\infty dp\,p^2\\
&\quad\times\left[\frac{n_\sigma}{\omega_\sigma}\frac{\omega_\psi^2+\omega_\sigma^2-k_0^2}{[k_0^2-(\omega_\psi-\omega_\sigma)^2][k_0^2-(\omega_\psi+\omega_\sigma)^2]}\right.\\
&\quad\left.+\frac{n_\psi}{\omega_\psi}\frac{2\omega_\psi^2}{[k_0^2-(\omega_\psi-\omega_\sigma)^2][k_0^2-(\omega_\psi+\omega_\sigma)^2]}\right],
\end{aligned}
\tag{B12}
$$

$$
(\Sigma_s^0)_\sigma=-\frac{g^2}{(4\pi)^2}m_\psi\left[\ln\left(\frac{m_\psi^2}{\mu^2}\right)+Z\right],
\tag{B13}
$$

$$
(\Sigma_0^0)_\sigma=-\frac{1}{(4\pi)^2}\frac{g^2}{2k_0}(k_0^2+m_\psi^2-m_\sigma^2)\left[\ln\left(\frac{m_\psi^2}{\mu^2}\right)+Z\right],
\tag{B14}
$$

with Z defined as

$$
Z\equiv\frac{1}{(4\pi)^2}\left[\frac{k_0^2+m_\sigma^2-m_\psi^2}{2k_0^2}\ln\left(\frac{m_\psi^2}{m_\sigma^2}\right)+\frac{\sqrt{\Delta_6}}{k_0^2}(\Delta_7+\Delta_8)\right],
\tag{B15}
$$

with $\Delta_6=k_0^4-2k_0^2(m_\psi^2+m_{\sigma;\pi}^2)+(m_\psi^2-m_{\sigma;\pi}^2)^2$, $\Delta_7=\operatorname{arctanh}\{[k_0^2+(m_\psi^2+m_{\sigma;\pi}^2)]/\sqrt{\Delta_6}\}$ and $\Delta_8=\operatorname{arctanh}[k_0^2-(m_\psi^2+m_{\sigma;\pi}^2)/\sqrt{\Delta_6}]$.

[1] M. Gell-Mann and M. Levy, Nuovo Cimento **16**, 705 (1960).
[2] D.H.T. Franco, H.C.G. Caldas, A.L. Mota, and M.C. Nemes, Mod. Phys. Lett. A **617**, 464 (1997), and references therein.
[3] L.R. Ram Mohan, Phys. Rev. D **14**, 2670 (1976).
[4] *Proceedings of Lattice 96* [Nucl. Phys. **B53**, 1 (1997)].
[5] *Proceedings of Quark Matter 97* [Nucl. Phys. **A638**, 1 (1998)].
[6] L. Dolan and R. Jackiw, Phys. Rev. D **9**, 3320 (1974).
[7] S. Weinberg, Phys. Rev. D **9**, 3357 (1974).
[8] A. Linde, Rep. Prog. Phys. **42**, 389 (1979); D.J. Gross, R.D. Pisarski, and L.G. Yaffe, Rev. Mod. Phys. **53**, 43 (1981).
[9] G. Baym and G. Grinstein, Phys. Rev. D **15**, 2897 (1977).
[10] N. Banerjee and S. Malik, Phys. Rev. D **43**, 3368 (1991).
[11] Rajesh R. Parwani, Phys. Rev. D **45**, 4695 (1992).
[12] S. Chiku and T. Hatsuda, Phys. Rev. D **58**, 076001 (1998).
[13] J. Kapusta, *Finite-Temperature Field Theory* (Cambridge University Press, Cambridge, England, 1989).
[14] B. Lee, *Chiral Dynamics* (Gordon and Breach, New York, 1970).
[15] D.A. Kirzhnits and A.D. Linde, Phys. Lett. **42B**, 471 (1972); Ann. Phys. (N.Y.) **101**, 195 (1976).
[16] G. Amelino-Camelia and S.-Y. Pi, Phys. Rev. D **47**, 2356 (1993).
[17] G. Amelino-Camelia, Phys. Rev. D **49**, 2740 (1994).
[18] H.-S. Roh and T. Matsui, Eur. Phys. J. A **1**, 205 (1998).
[19] N. Petropoulos, J. Phys. G **25**, 2225 (1999).

[20] P. Ramond, *Field Theory: A Modern Primer* (Addison Wesley, New York, 1990).
[21] C.W. Bernard, Phys. Rev. D **9**, 3312 (1974).
[22] A. Bochkarev and J.I. Kapusta, Phys. Rev. D **54**, 4066 (1996).
[23] P.V. Landshoff, hep-ph/9808362.
[24] M. Chanowitz, M. Furman, and I. Hinchliffe, Nucl. Phys. **B159**, 225 (1979).
[25] Peter Arnold and Olivier Espinosa, Phys. Rev. D **47**, 3546 (1993).
[26] J.M. Cornwall, R. Jackiw, and E. Tomboulis, Phys. Rev. D **10**, 2428 (1974); G. Amelino-Camelia and S.-Y. Pi, *ibid.* **47**, 2356 (1993).
[27] G. Amelino-Camelia, Phys. Lett. B **407**, 268 (1994).
[28] J.T. Lenaghan and D.H. Rischke, J. Phys. G **26**, 431 (2000).
[29] F. Karsch, A. Patks, and P. Petreczky, Phys. Lett. B **401**, 69 (1997).
[30] H.C.G. Caldas, D.H.T. Franco, A.L. Mota, F.A. Oliveira, and M.C. Nemes, Nucl. Phys. **A617**, 464 (1997).
[31] J. Randrup, Phys. Rev. D **55**, 1188 (1997).
[32] N. Bilic and H. Nikolie, Eur. Phys. J. C **6**, 513 (1999).
[33] P.K. Panda, A. Mishra, J.M. Eisemberg, and W. Greiner, Phys. Rev. C **56**, 3134 (1997).